MULTI-RATE DIGITAL REDESIGN OF CASCADED AND DYNAMIC OUTPUT FEEDBACK SYSTEMS

A Thesis

Presented to

the Faculty of the Department of Electrical and Computer Engineering

University of Houston

In Partial Fulfillment

of the Requirements for the Degree

Master of Science

in Electrical and Computer Engineering

by

Selim A. Özkul

May 2012

ACKNOWLEDGEMENTS

I would like to express my sincere thanks to my advisor, Dr. Leang San Shieh, for his valuable guidance, unconditional support and enthusiastic encouragement throughout my graduate studies at the University of Houston. Working with him has been a great learning experience.

I am highly indebted to my thesis committee members for their valuable suggestions and constructive criticism that have added depth and enriched the scope of this study. Special thanks go to my dearest friends for always being supportive in every way possible. It is not possible to mention all of them here.

Finally, my deepest gratitude goes to my family, especially to my parents, for their constant love and encouragement. Even though they were far away from me in another continent, they were always in my heart. Hearing their voices and suggestions meant a lot to me. I would like to dedicate this thesis to my mother and father, Dr. Emine Ozkul and Dr. Osman Sadi Ozkul, whose experiences motivated me along this challenging journey. Simply, I would not be where I am right now without you. Thank you very much!

MULTI-RATE DIGITAL REDESIGN OF CASCADED AND DYNAMIC OUTPUT FEEDBACK SYSTEMS

An Abstract

of a

Thesis

Presented to

the Faculty of the Department of Electrical and Computer Engineering

University of Houston

In Partial Fulfillment

of the Requirements for the Degree

Master of Science

in Electrical and Computer Engineering

by

Selim A. Özkul

May 2012

ABSTRACT

In this research, new indirect digital redesign methods are presented for multi-rate sampled control systems with cascaded and dynamic output feedback controllers. Unlike the classical direct bilinear transform, which is an open-loop direct digital redesign method, the proposed digital controllers take into account the state-matching of the original continuous-time closed-loop system and the digitally redesigned sampled-data closed-loop system. Direct bilinear transform is a fairly simple method that has been widely used in industry for a long time. However, it ignores the continuous-time controllers and plant as a complete system and treats all of the controllers individually. Generally, this method might be good for short sampling periods, however the system response might become unstable for longer sampling periods. Therefore, closed-loop digital redesign methods are preferred while calculating digital controllers.

Analog controllers are often predesigned based on a desirable frequency specification, such as the bandwidth, the natural angular frequency, etc. To take advantage of the digital controllers over the analog controllers, digital implementation of analog controllers is often desirable. However, continuous-time system states might not be readily available. Therefore, an ideal state reconstructing algorithm was utilized to obtain the multi-rate discrete-time states of the original continuous-time system. By utilizing these obtained states and applying Chebyshev quadrature method, improved digital redesign method and lifting methods, multi-rate cascaded and dynamic output feedback digital controllers were constructed. Illustrative examples are provided to demonstrate the effectiveness of the developed methods.

TABLE OF CONTENTS

LIST OF FIGURES

CHAPTER 1 - INTRODUCTION

Most practical and industrial processes often consist of continuous-time (analog) actuators and sensors with specific characteristics. To improve the performance of the overall systems, the cascaded analog controller, such as the proportional-integral-derivative (PID) controller [2-3], and the dynamic output feedback controller, such as the bending filter [10] are usually designed.

The designed closed-loop continuous-time controllers are usually required to be converted into their discrete-time (digital) forms for the purpose of analysis and digital implementation of the controllers. Digital controllers implemented using digital processors cost less, have a smaller size and offer better performance.

The existing approximate methods to formulate digital counterparts of the continuous-time controllers are based on assumptions. Direct bilinear transformation method simply substitutes the controllers into digital forms using ($s = \frac{2(z-1)}{T(z+1)}$), which does not take state matching into consideration. Moreover this method is considered an open loop design. Further improved design considers using a closed-loop bilinear redesign method which improves the system response; however system response becomes unstable for small sampling rates.

Plants with various sensor measurements and time constants led scientists to develop new solutions to accommodate different rates of data. Radar, airplanes, satellites, internet based control systems [16,27] and hard disk drives are examples to be considered. This aspect gave birth to multi-rate sampling techniques for hybrid control of the continuous-time systems. There are different types of control structures, which can

be divided basically into two classes. One is a multi-rate closed-loop system with a slow-rate cascaded controller and a fast-rate output-feedback controller, and the other one is a multi-rate closed-loop system with a fast-rate cascaded controller and a slow-rate output-feedback controller. In hard disk driver and internet-based control systems, the feed-forward controller is sampled at a fast-rate and the feedback controller is updated at a slow-rate [15].

In this research, a new indirect multi-rate digital redesign method is developed for the control systems with both cascaded and dynamic output feedback controllers. The state variables are not readily available to the controllers, so an ideal state reconstructing technique is utilized to compute the discrete-time states of the continuous-time controller. New techniques are formulated such as the Chebyshev quadrature method [21] and the improved digital redesign method to construct the cascaded and dynamic output feedback digital controllers. Also, using different sampling rates the controllers are designed and combined together to achieve a multi-rate hybrid control of the continuous-time systems.

1.1 Outline of the Research

This research consists of six chapters. Chapter 1 provides an introduction to the research subject. The outline and the objective of this research and the review of previous works are also presented.

Chapter 2 gives a brief description of the analytical models used in this study. New approximation methods such as the Chebyshev quadrature method and the improved digital redesign methods are formulated. Modeling errors are compared among different

methods. The newly developed approximation methods are compared with existing solution methods such as direct bilinear method in the end.

Chapter 3 presents a brief description of N-delay control; the lifting method is improved for the digital redesign method used in this study. Chapter 4 presents the multi-rate digital redesign method. The multi-rate digital redesign method is formulated for plants with feedback and feed-forward gains. Different digital controller gains are calculated for various sampling times. Also, an ideal digital state reconstructor [17] is presented.

Chapter 5 provides illustrative examples for both systems with and without input time delays. Simulation results from the digital redesign method are compared with the actual system response and each method is compared. Lastly, Chapter 6 gives a summary and conclusions of this study. Possible future work is also mentioned in this chapter.

1.2 Review of Previous Work

Procedures for formulating and simulating multi-rate digital redesign started to be developed in the past 50 years. In most of the methods developed by researchers, methods became very complex and hard to calculate whenever the ratio of slow to fast sampling ratio increases. Studies related to this subject since the 1950s are briefly summarized below.

Multi-rate digital controller design has been the interest of the researchers since the 1950's and different approaches have been developed ever since [1,4-6,8-9,11-15,19,21,23,26]. Due to recent developments in digital processors it is necessary to use digital controllers and implement them. Early stages of multi-rate design start with the

frequency decomposition technique followed by the switch decomposition technique. Later, Kalman and Bertram show that state space techniques provide good results in characterizing sampled-data systems. Both of these techniques are shown to be equivalent later. However, there is a major disadvantage for both of these techniques. The analysis and synthesis become complex when the fast-rate and slow-rate sampling ratio increases [3,12]. A new indirect multi-rate digital redesign method is developed in this research for both cascaded and output-feedback systems and examples are provided to show this method can be used in different applications.

1.3 Research Objectives

The main purpose of this study is to develop a new method for multi-rate digital redesign control systems with and without input delays. The specific objectives are as follows:

1) Develop a new method to calculate digital gains of feedback and feedforward based on their continuous-time controller counterparts.
2) Compare the existing methods with developed methods that are proposed in this research (qualitative and quantitative comparison).

CHAPTER 2 - PROBLEM FORMULATION AND DIGITAL REDESIGN METHODS WITH NO INPUT DELAY

Consider a controllable and observable linear continuous-time control system with a cascaded and a dynamic output feedback controller depicted in Figure 2-1, where $G_1(s)$ is the continuous-time plant; $G_2(s)$ and $G_3(s)$ are the continuous-time cascaded and the output feedback controllers. The state space models of $G_1(s)$, $G_2(s)$ and $G_3(s)$ are (A_1, B_1, C_1, D_1), (A_2, B_2, C_2, D_2) and (A_3, B_3, C_3, D_3), $r(t)$ is the reference input and E_c is the forward gain. The state dimensions, input and output numbers of $G_1(s)$, $G_2(s)$ and $G_3(s)$ are (n_1, m_1, p_1), (n_2, m_2, p_2) and (n_3, m_3, p_3), respectively.

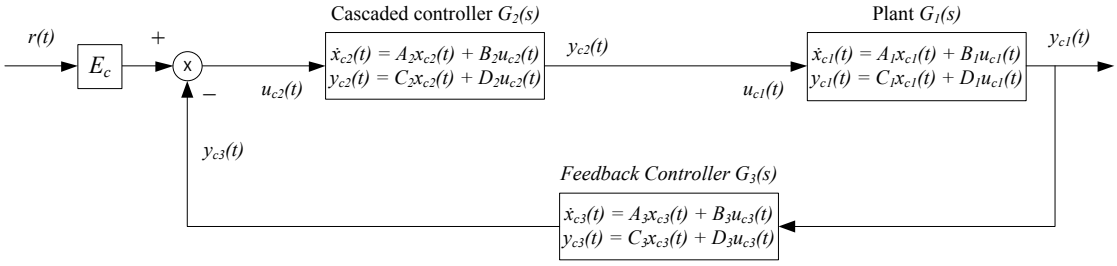

Figure 2-1. Continuous-time closed-loop system

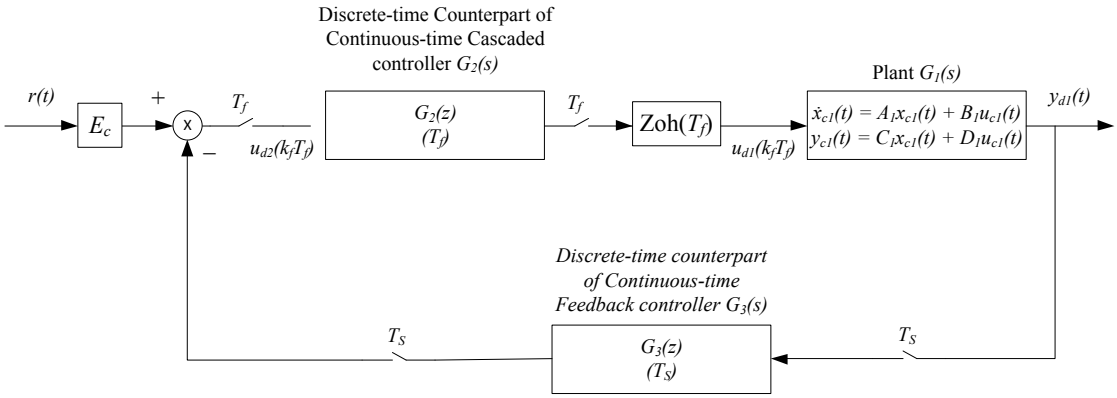

Figure 2-2. Classical multi-rate sampling control system

Without loss of generality, we assume $D_1 = 0$. One of the classical multi-rate sampling control structures for the original continuous-time system $G_1(s)$, is depicted in Figure 2-2, where $G_2(z)$ and $G_3(z)$ are digital controllers of $G_2(s)$ and $G_3(s)$. T_f and T_s are noted as the fast-rate and slow-rate sampling time periods, respectively. $T_s = NT_f$, where *N* is a positive integer. Moreover, $Zoh(T_f)$ denotes a zero-order hold with holding time T_f. The subscript "c" in the functions $x_{c1}(t)$ and $y_{c1}(t)$ in Figure 2.1 designates the continuous-time functions controlled by the continuous-time signal $u_{c1}(t)$. Whereas the subscript "*d*" in the functions $x_{d1}(t)$ and $y_{d1}(t)$ in Figure 2.2 denotes the continuous-time functions controlled by the discrete-time signal $u_{d1}(k_f T_f)$.

As described in Chapter 1, the other classical multi-rate sampling control structure is that the slow-rate sampling period T_s is used in a cascaded controller $G_2(s)$, and fast-rate sampling period T_f is employed in the output feedback controller $G_3(s)$. The proposed multi-rate digital redesign problem is that if we are given the analog controllers $G_2(s)$, $G_3(s)$ and the gain E_c with the multi-rate sampling periods T_s and T_f, how can we find the equivalent digital controllers and gain from $G_2(s)$, $G_3(s)$ and E_c so that the states or outputs of the digitally controlled plant $G_1(s)$ closely match those of the plant $G_1(s)$ with the analog controller.

2.1 Digital Redesign Method

Two figures and the following equations below indicate the basic of design. As indicated in Figure 2-3, K_c and E_c are formerly calculated values to satisfy the desired conditions (settling time, peak value, rise time etc…) of the output value $y_c(t)$. As shown on Figure 2-4, K_d and E_d are the discrete-time equivalent counterparts of K_c and

E_c. K_d and E_d are calculated to implement cascaded and feedback controls in microprocessors and digital signal processors to acquire the same output and conditions. K_d and E_d will be calculated using K_c and E_c, state matching equations. Hence, the digital redesign of the system will be completed.

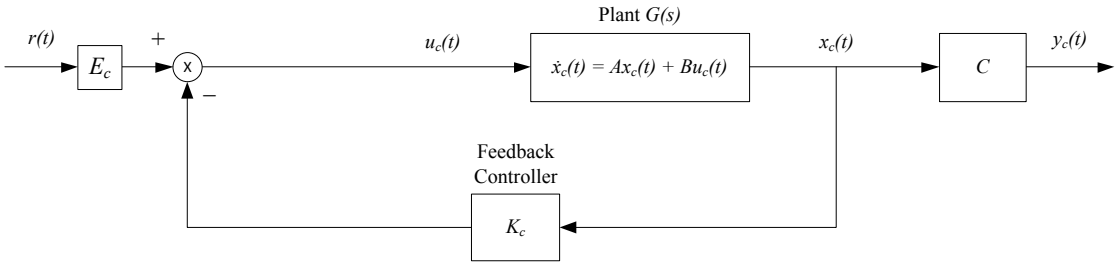

Figure 2-3. Continuous-time closed-loop system with continuous-time state feedback

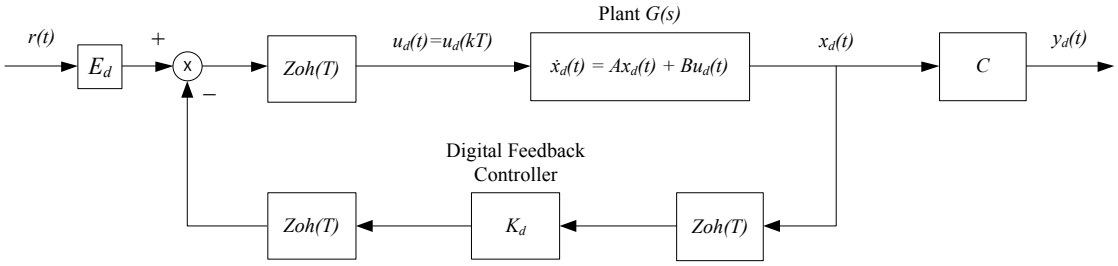

Figure 2-4. Continuous-time closed-loop system with discrete-time state feedback

Consider the state-space model of a dynamic system *G(s)* as shown in Figure 2-3 as

$$\dot{x}_c(t) = Ax_c(t) + Bu_c(t), x_c(0) = x_{co}, \tag{2-1}$$

$$y_c(t) = Cx_c(t), \tag{2-2}$$

where $x_c(t) \in R^{nx1}$, $u_c(t) \in R^{mx1}$, $y_c(t) \in R^{px1}$ are system state, input and output vector, respectively. x_{c0} is the initial condition and analog controller is

$$u_c(t) = -K_c x_c(t) + E_c r(t), \tag{2-3}$$

where $r(t) \in R^{mx1}$ is the reference input, $K_c \in R^{mxn}$, $E_c \in R^{mxm}$ are the analog feedback and feed-forward gains. Substituting equation (2-3) into (2-1) results in the closed-loop system

$$\dot{x}_c(t) = Ax_c(t) + B[-K_c x_c(t) + E_c r(t)], \tag{2-4}$$

$$\dot{x}_c(t) = A_c x_c(t) + BE_c r(t), \tag{2-5}$$

where $A_c = A - BK_c$.

The corresponding designed, discrete-time exact evaluation of the closed loop continuous-time system becomes the following:

$$x_c(kT + T) = e^{A_c T} x_c(kT) + \int_{kT}^{kT+T} e^{A_c(kT+T-\lambda)} BE_c r(\lambda) d\lambda, \tag{2-6}$$

$$x_c(kT + T) = G_c x_c(kT) + H_c E_c r(kT), \tag{2-7}$$

where $G_c = e^{A_c T}$, $H_c = \int_{kT}^{kT+T} e^{A_c(kT+T-\lambda)} B d\lambda = [G_c - I_n] A_c^{-1} B$, I_n is the identity matrix with dimension n, and $r(t) = r(kT)$ for $kT \leq t < (k+1)T$.

Consider the digitally controlled hybrid system which approximates the states of the continuous-time system in Figure 2-4 as

$$\dot{x}_d(t) = Ax_d(t) + Bu_d(kT), \tag{2-8}$$

$$y_d(t) = \mathrm{C}x_d(t), \tag{2-9}$$

with a digital controller

$$u_d(kT) = -K_d x_d(kT) + E_d r(kT), \text{ for } kT \le t \le kT + T \tag{2-10}$$

where T is the sampling period, $K_d \in R^{mxn}$, $E_d \in R^{mxm}$ are the discrete-time state feedback and state forward gains. Although equation (2-8) is a hybrid system, it is still a continuous-time signal and the corresponding discrete-time model becomes

$$x_d(kT + T) = e^{AT}x_d(kT) + \int_{kT}^{kT+T} e^{A(kT+T-\lambda)}Bd\lambda * u_d(kT) \tag{2-11}$$

which can be written such as

$$x_d(kT + T) = Gx_d(kT) + Hu_d(kT), \tag{2-12}$$

where $G = e^{AT}$, $H = \int_{kT}^{kT+T} e^{A(kT+T-\lambda)}Bd\lambda = [G - I_n]A^{-1}B$ for a non-singular matrix A. When the matrix A is a singular matrix, the matrix H can be evaluated as

$$H = \sum_{i=1}^{\infty} \frac{T}{i!}(AT)^{i-1}B \tag{2-13}$$

above. Now that equation (2-12) is represented in its discrete-time, inserting equation (2-10) into equation (2-12) becomes the closed-loop equation, which is

$$x_d(kT+T) = (G - HK_d)x_d(kT) + HE_d r(kT) \tag{2-14}$$

above. Two closed-loop systems has been calculated in equations (2-7) and (2-14) so far. In this research, the discrete-time system is matched at every sampling period with the continuous-time system. State matching conditions are shown below,

$$x_c(t)|_{t=kT+T} = x_d(t)|_{t=kT+T}, \tag{2-15}$$

$$x_c(t)|_{t=kT} = x_d(t)|_{t=kT}. \tag{2-16}$$

Based on state matching equations above and using equations (2-7) and (2-14), the following equations are deduced,

$$G_c = G - HK_d, \tag{2-17}$$

$$H_c E_c = HE_d. \tag{2-18}$$

However, as it can be understood, there is not an exact solution to the equations above. In these circumstances, approximate solutions are researched. In the following sections different approximations are researched and explained.

2.2 Chebyshev's Bilinear Transform Method for Feedback Systems

The Chebyshev quadrature method is a good approximation to calculate digital control gains K_d, and E_d. A revision of the discrete-time model of the equation (2-1), similar to equation (2-11), can be rewritten as

$$x_c(kT+T) = Gx_c(kT) + \int_{kT}^{kT+T} e^{A(kT+T-\lambda)} Bu_c(\lambda)d\lambda \tag{2-19}$$

Consider the Chebyshev quadrature formula

$$\begin{aligned}\int_a^b \omega(\lambda)f(\lambda)d\lambda &= \int_a^b \omega(\lambda)d\lambda \cdot \lim_{N\to\infty}\left(\frac{1}{N+1}\right)\sum_{i=0}^{N} f(\lambda_i) \\ &= \int_a^b \omega(\lambda)d\lambda \cdot \lim_{N\to\infty}\left(\frac{N}{(N+1)(b-a)}\right)\sum_{i=0}^{N} f(\lambda_i)\frac{(b-a)}{N} \\ &= \int_a^b \omega(\lambda)d\lambda \cdot \frac{1}{b-a}\int_a^b f(\lambda)d\lambda, \end{aligned} \tag{2-20}$$

where $\omega(\lambda)$ is a constant sign weighting function in $[a,b]$ and $f(\lambda_i)$ are the values of the function $f(\lambda)$ evaluated at $\lambda = a + i(b - a/N)$, for $i = 0, 1, \ldots, N$. The above result can be utilized to approximately evaluate the integral term in equation (2-19) as

$$\int_{kT}^{kT+T} e^{A(kT+T-\lambda)} Bu_c(\lambda)d\lambda \cong \frac{1}{T}\int_{kT}^{kT+T} e^{A(kT+T-\lambda)} Bd\lambda \int_{kT}^{kT+T} u_c(\lambda)\, d\lambda. \tag{2-21}$$

So the following is obtained

$$\hat{x}_c(kT+T) = G\hat{x}_c(kT) + Hu_d(kT), \tag{2-22}$$

where $u_d(kT) = \frac{1}{T}\int_{kT}^{kT+T} u_c\,(\lambda)d\lambda$ and $\hat{x}_c(kT)$ in equation (2-22) is an approximate state of $x_c(kT)$ in (2-19). Substituting equation (2-3) into (2-22) results in

$$\hat{x}_c(kT+T) = G\hat{x}_c(kT) + H\frac{1}{T}\int_{kT}^{kT+T}(-K_c\hat{x}_c(\lambda) + E_c r(\lambda))d\lambda. \quad (2\text{-}23)$$

Applying the trapezoidal rule integration to the integral term in equation (2-23), it is obtained that $\frac{1}{T}\int_{kT}^{kT+T}\hat{x}_c(\lambda)d\lambda \cong \frac{1}{2}(\hat{x}_c(kT+T) + \hat{x}_c(kT))$. As a result, equation (2-23) becomes

$$\hat{x}_c(kT+T) = \left(I_N + \frac{1}{2}HK_c\right)^{-1}\left(G - \frac{1}{2}HK_c\right)\hat{x}_c(kT) + \left(I_N + \frac{1}{2}HK_c\right)^{-1}HE_c r(kT). \quad (2\text{-}24)$$

To match the closed-loop states in equations (2-14) and (2-24), states of both systems must match at every sampling period, resulting in the following conditions,

$$\hat{x}_c(t)|_{t=kT+T} = x_d(t)|_{t=kT+T} \; and \; \hat{x}_c(t)|_{t=kT} = x_d(t)|_{t=kT}. \quad (2\text{-}25)$$

As a result of the above condition, the following equations are solved for K_d and E_d,

$$G - HK_d = \left(I_n + \frac{1}{2}HK_c\right)^{-1}\left(G - \frac{1}{2}HK_c\right), \quad (2\text{-}26)$$

$$HE_d = \left(I_n + \frac{1}{2}HK_c\right)^{-1}HE_c. \quad (2\text{-}27)$$

Using Chebyshev's bilinear transformation method the equations shown above can be solved and the result K_d and E_d values are as follows,

$$K_d = \frac{1}{2}\left(I_m + \frac{1}{2}K_c H\right)^{-1} K_c(I_n + G), \tag{2-28}$$

$$E_d = (I_m + \frac{1}{2}K_c H)^{-1} E_c, \tag{2-29}$$

where $H \in R^{nxm}$, $G \in R^{nxn}$ and $K_c \in R^{mxn}$.

Remark 1: Based on the Chebyshev quadrature formula in equation (2-21), when $u_c(\lambda)$ in equation (2-21) is a piecewise constant signal, the integral term in the left-hand side of equation (2-21) is exactly equal to the product of the two integral term in the right-hand side of equation (2-21). Otherwise, the approximation error in (2-21) is proportional to the square of the sampling period T [18]. In addition, from equation (2-19) and (2-22), the digital control law $u_d(kT) = \frac{1}{T}\int_{kT}^{kT+T} u_c(t)dt$ is the average area under the curve $u_c(t)$ from kT to $(kT + T)$, as depicted in Figure 2-5. As a result, when the $u_c(t)$ is a piecewise linear time-varying signal, the value of $u_d(kT)$ becomes the average of $u_c(t)$ at $t = kT + T$ and $u_c(t)$ at $t = kT$ obtained by the trapezoidal rule or the bilinear transform method. Substituting the $u_c(t)$ in equation (2-3) into the $u_d(kT)$ in (2-22) results in the indirect digital control gains in equations (2-28) and (2-29). The digital control law $u_d(kT)$ in equation (2-22) with the gains in (2-28) and (2-29) can be referred to as the closed-loop bilinear transformed controller.

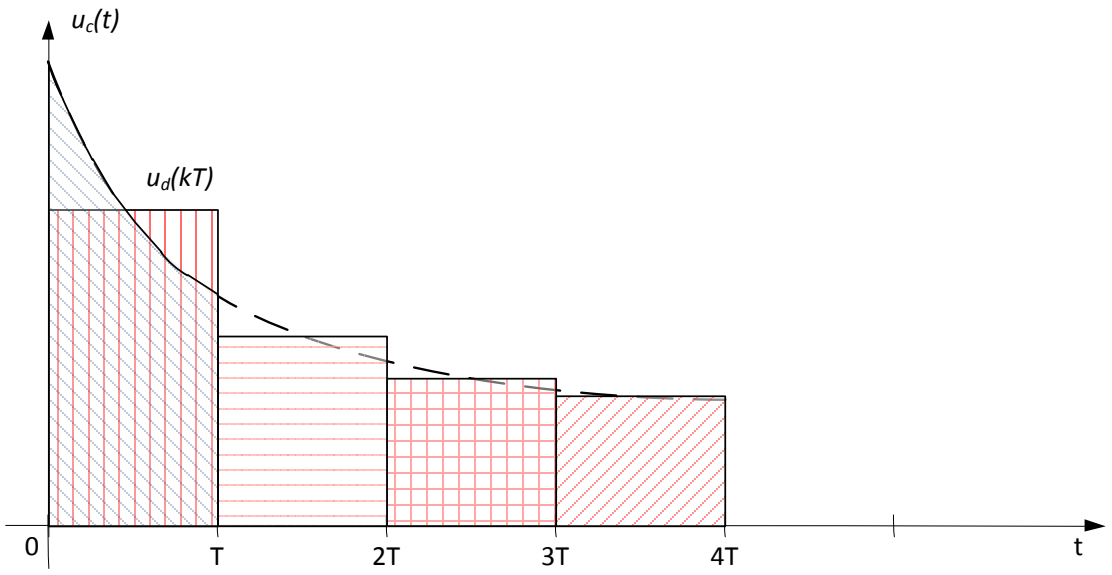

Figure 2-5. Analog control $u_c(t)$ and digital control $u_d(kT)$

2.3 Improved digital redesign method

A better approach to evaluate digital control gains K_d and E_d is improved digital redesign method. The method differs from Chebyshev bilinear method by exactly evaluating $\int_{kT}^{kT+T} x_c(\lambda)d\lambda$ in equation (2-23).

$u_d(kT)$ equation (2-23) can be written as

$$u_d(kT) = \frac{1}{T}\int_{kT}^{kT+T} u_c(\lambda)d\lambda = -\frac{K_c}{T}\int_{kT}^{kT+T} x_c(\lambda)d\lambda + E_c r(kT) \qquad (2\text{-}30)$$

shown above. The integral term on the right-hand side of equation (2-30) can be exactly evaluated by integrating the analog designed system shown in equation (2-5), as a result the following results are obtained

$$\int_{kT}^{kT+T} \dot{x}_c(t)dt = A_c \int_{kT}^{kT+T} x_c(\lambda)d\lambda + BE_c \int_{kT}^{kT+T} r(\lambda)d\lambda, \quad (2\text{-}31)$$

$$\int_{kT}^{kT+T} \dot{x}_c(t)dt = \int_{kT}^{kT+T} dx_c(t) = x_c(kT+T) - x_c(kT), \quad (2\text{-}32)$$

then it follows as

$$\int_{kT}^{kT+T} x_c(t)dt = A_c^{-1}[x_c(kT+T) - x_c(kT) - TBE_c r(kT)], \quad (2\text{-}33)$$

where $r(t) = r(kT)$ for $kT \leq t < kT+T$.

Utilizing equation (2-7) into equation (2-33) and solving for $\int_{kT}^{kT+T} x_c(\lambda)d\lambda$ leads to the following

$$\int_{kT}^{kT+T} x_c(\lambda)d\lambda = A_c^{-1}[G_c x_c(kT) + H_c E_c r(kT) - x_c(kT) - BE_c T r(kT)], \quad (2\text{-}34)$$

$$\int_{kT}^{kT+T} x_c(\lambda)d\lambda = A_c^{-1}[(G_c - I_n)x_c(kT) + (H_c - BT)E_c r(kT)], \quad (2\text{-}35)$$

equations above. Letting $x_c(t)$ in equation (2-35) as $\hat{x}_c(t)$, $x_c(kT) = \hat{x}_c(kT)$ and $x_c(kT+T) = \hat{x}_c(kT+T)$, also substituting equation (2-35) into (2-30)

$$u_d(kT) = -\frac{K_c}{T} \int_{kT}^{kT+T} \hat{x}_c(\lambda)d\lambda + E_c r(kT),$$

$$u_d(kT) = -\frac{K_c}{T}\left[A_c^{-1}[(G_c - I_n)\hat{x}_c(kT) + (H_c - BT)E_c r(kT)]\right] + E_c r(kT),$$

$$u_d(kT) = -[K_c(A_cT)^{-1}(G_c - I_n)]\hat{x}_c(kT) + [K_c(A_cT)^{-1}(BT - H_c) + I_m]E_c r(kT), \quad (2\text{-}36)$$

results in the digitally redesigned input signal.

Comparing equations (2-10) and (2-36) leads to the following cascaded and feedback digital controller gains K_d and E_d to be

$$K_d = K_c(A_cT)^{-1}(G_c - I_n), \quad (2\text{-}37)$$

$$E_d = [K_c(A_cT)^{-1}(BT - H_c) + I_m]E_c. \quad (2\text{-}38)$$

The corresponding digitally redesigned method is called as the improved bilinear transform method.

2.4 Direct bilinear transform method

The commonly used digital redesign method in industry is the direct bilinear transform, which could convert the predesigned cascaded and output feedback continuous-time controllers directly into their digital forms, however it fails to convert a state-feedback controller into digital form. Unlike, the other methods described in this research, the direct bilinear transform method does not take state matching into consideration. Although its structure is simple, the stability of the closed-loop sampled-date system is not assured if the sampling time is set too large. The digital control systems using the direct bilinear transform method are achieved as follows.

Suppose $G_1(s)$ is the transfer function of the continuous-time system in Figure 2-1, then the digital form of $G_1(s)$ is

$$G_1(z) = G_1(z)\big|_{s=\frac{2(Z-1)}{T(Z+1)}}, \tag{2-39}$$

where the respective variables s and z denote the continuous-time and discrete-time operators, and T is denoted as the sampling period.

On the other hand, the continuous-time system $G_1(s)$ is represented by equation (2-1), then the state-space model under the bilinear transform is

$$x_b(kT+T) = G_b x_b(kT) + H_b u(kT), \tag{2-40}$$

$$y_b(kT) = C x_b(kT), \tag{2-41}$$

where $G_b = \left(I_n - \frac{AT}{2}\right)^{-1}(I_n + \frac{AT}{2})$, $H_b = (I_n - \frac{AT}{2})^{-1}BT$, $x_b(kT)$ is the discrete-time state of $x_c(t)$ evaluated at $t = kT$ for $k = 0, 1, 2, \cdots$. For modeling error analysis, let the modeling error matrices be $E_g = e^{AT} - G_b$ and $E_b = (G - I_n)A^{-1}B - (I_n - \frac{1}{2}AT)^{-1}BT$, then the modeling errors between the bilinear transform method represented by equations (2-40) and (2-41) and the exact discrete-time model of equation (2-1) become

$$\|E_g\| \le \sum_{i=1}^{\infty}\left(\frac{1}{2^{i-1}} - \frac{1}{i!}\right)\|(AT)^i\| = \frac{1 + 0.5\|AT\|}{1 - 0.5\|AT\|} - e^{\|AT\|},$$

$$\|E_b\| \le \|E_g\|\|A^{-1}B\| \le \|E_g\|\|A^{-1}\|\|B\|,$$

for $T \le \frac{2}{\|A\|}$ and a non-singular matrix A, where $\|A\|$ is the Euclidean norm of A. The evaluation of the modeling error $\|E_b\|$ for the singular matrix A is given in the appendix A.

CHAPTER 3 - DIGITAL REDESIGN TECHNIQUE FOR STABLE AND UNSTABLE SYSTEMS USING LIFTING METHOD

3.1 N-Delay Control

Another approach that can be utilized is the N-delay lifting technique. Using this technique the input matrix can be adjusted, so that the state variables are exactly matched and there is no approximation.

3.1.1 Introduction to Lifting Technique

Consider the input signal shown below in Figure 3-1. The input signal is sampled with a sampling period of T_f as shown in Figure 3-2 and the output signal becomes as shown in Figure 3-3.

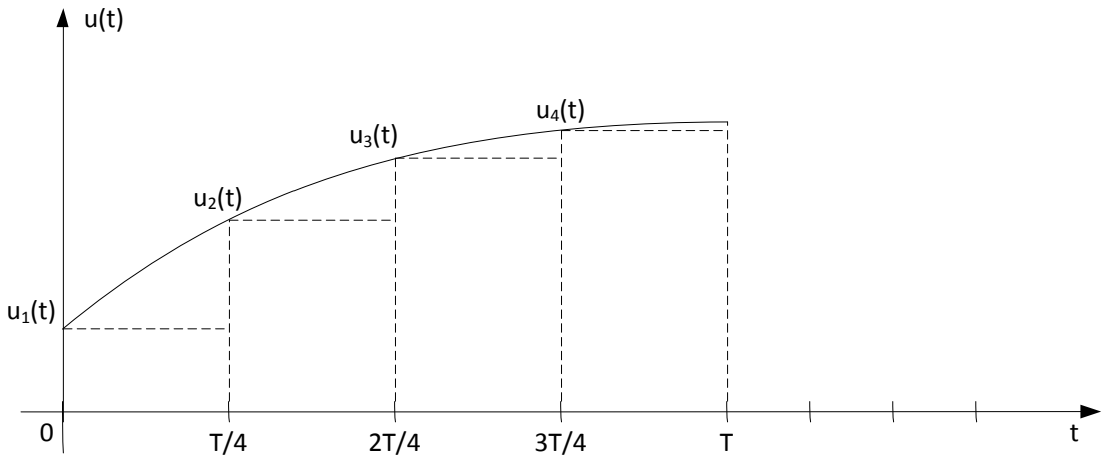

Figure 3-1. Continuous-time signal

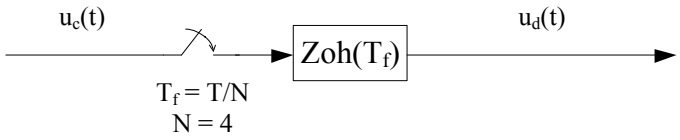

Figure 3-2. Continuous-time signal via zero-order hold

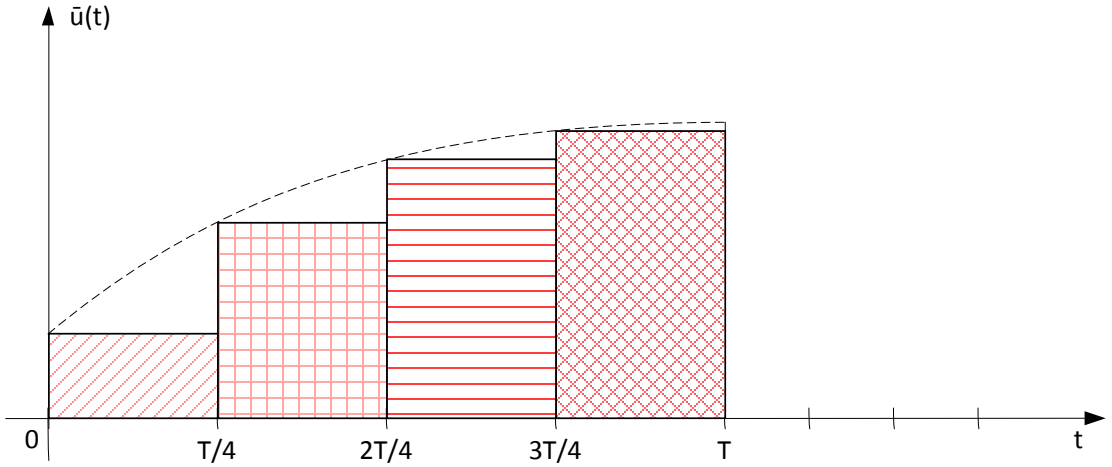

Figure 3-3. Sampled output signal

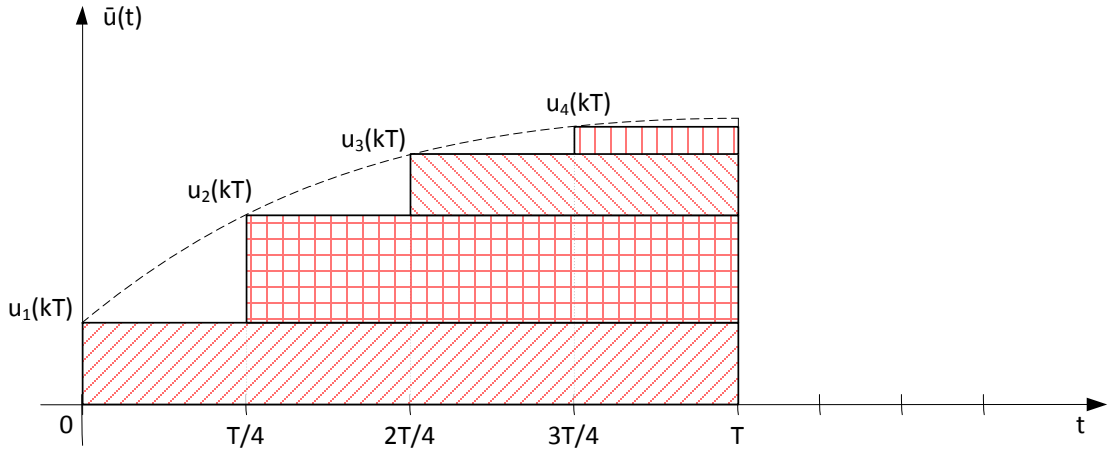

Figure 3-4. Output signal series to parallel conversion

The output signal can also be represented as shown in Figure 3-4. Although, the Figure 3-3 and Figure 3-4 representations indicate the same signal, the analytic representation can be shown below,

$$\overrightarrow{u} = \begin{bmatrix} u_1(kT) \\ u_2(kT) \\ u_3(kT) \\ u_4(kT) \end{bmatrix} = \begin{bmatrix} u(kT) \\ u(kT + \frac{T}{4}) \\ u(kT + \frac{2T}{4}) \\ u(kT + \frac{3T}{4}) \end{bmatrix} \cong u(t). \tag{3-1}$$

Consider the state-space representation of a continuous-time plant below

$$\dot{x}(t) = Ax(t) + Bu(t), \tag{3-2}$$

$$y(t) = Cx(t) + Du(t). \tag{3-3}$$

Transfer function of the system shown in equations (3-3) and (3-4) can be represented as

$$G(s) = C(sI_n - A)^{-1}B + D. \tag{3-4}$$

Figure 3-2 represent s an input signal sampled with $T/4$ zero-order hold and as a result, Figure 3-3 is obtained. However, using the lifting method, the series components are substituted with parallel signals as shown on Figure 3-4. However, such a conversion cannot be achieved by the zero-order hold circuit as shown in Figure 3-2. A simple block diagram expressing a continuous-time signal as a discrete-time signal using the lifting method is shown in Figure 3-5 below.

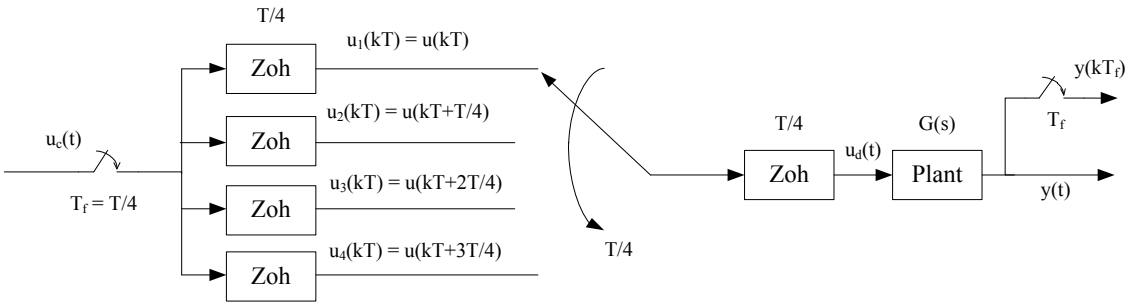

Figure 3-5. Discrete-time representation of plant using lifting method

The counterpart equivalent discrete-time representation of a continuous-time plant as shown in equations (3-2) and (3-3) can be calculated as

$$x(kT+T) = e^{AkT}x(kT) + \int_{kT}^{kT+T} e^{A(kT+T-\tau)}Bu_1(\tau)d\tau\,,$$

$$+ \int_{kT+\frac{T}{4}}^{kT+T} e^{A(kT+T-\tau)}B[u_2(\tau)-u_1(\tau)]d\tau\,,$$

$$+ \int_{kT+\frac{2T}{4}}^{kT+T} e^{A(kT+T-\tau)}B[u_3(\tau)-u_2(\tau)]d\tau\,,$$

$$+ \int_{kT+\frac{3T}{4}}^{kT+T} e^{A(kT+T-\tau)}B[u_4(\tau)-u_3(\tau)]d\tau. \qquad (3\text{-}5)$$

From Figure 3-4, the input signals are observed to be constant during the above time intervals, also the B matrices are constant, so the equations can be written as follows,

$$x(kT+T) = e^{AkT}x(kT) + \int_{kT}^{kT+T} e^{A(kT+T-\tau)}d\tau\, Bu_1(\tau),$$

$$+ \int_{kT+\frac{T}{4}}^{kT+T} e^{A(kT+T-\tau)}d\tau\, Bu_2(\tau) - \int_{kT+\frac{T}{4}}^{kT+T} e^{A(kT+T-\tau)}d\tau\, B\,u_1(\tau)\,,$$

$$+\int_{kT+\frac{2T}{4}}^{kT+T} e^{A(kT+T-\tau)}d\tau\, Bu_3(\tau) - \int_{kT+\frac{2T}{4}}^{kT+T} e^{A(kT+T-\tau)}d\tau\; u_2(\tau),$$

$$+\int_{kT+\frac{3T}{4}}^{kT+T} e^{A(kT+T-\tau)}d\tau\, Bu_4(\tau) - \int_{kT+\frac{3T}{4}}^{kT+T} e^{A(kT+T-\tau)}d\tau\, Bu_3(\tau). \quad (3\text{-}6)$$

Solving the integrals in equation (3-6), further simplifies the above equations to be expressed as

$$x(kT+T) = Gx(kT) + (H_1 - H_2)u_1(kT) + (H_2 - H_3)u_2(kT)$$
$$+ (H_3 - H_4)u_3(kT) + H_4u_4(kT)\,, \quad (3\text{-}7)$$

$$x(kT+T) = (G_4)^4x(kT) + [(G_4)^3H_4, (G_4)^2H_4, (G_4)^1H_4, H_4]\begin{bmatrix}u_1(kt)\\u_2(kt)\\u_3(kt)\\u_4(kt)\end{bmatrix}, \quad (3\text{-}8)$$

where $G_4 = e^{A\frac{T}{4}}$, $G_N = e^{A\frac{T}{N}}$ and $H_N = [G_N - I]A^{-1}B$.

Based on the discrete-time state variables of the N-delay lifted system represented in (3-8), the discrete-time output can be expressed as

$$\begin{bmatrix}y_1(kT)\\y_2(kT)\\y_3(kT)\\y_4(kT)\end{bmatrix} \triangleq \begin{bmatrix}y(kT)\\y\left(kT+\frac{T}{4}\right)\\y\left(kT+\frac{2T}{4}\right)\\y\left(kT+\frac{3T}{4}\right)\end{bmatrix} = \begin{bmatrix}C\\CG_4^1\\CG_4^2\\CG_4^3\end{bmatrix}x(kT) + \begin{bmatrix}D & 0 & 0 & 0\\CH_4 & D & 0 & 0\\CG_4^1H_4 & CH_4 & D & 0\\CG_4^2H_4 & CG_4^1H_4 & CH_4 & D\end{bmatrix}\begin{bmatrix}u_1(kT)\\u_2(kT)\\u_3(kT)\\u_4(kT)\end{bmatrix}, \quad (3\text{-}9)$$

where the system becomes a multi-input multi-output (MIMO) system.

3.2 Digital Redesign Using the Lifting Method

Although digital control law developed using the improved digital method, the redesign method utilizes the exact integral term of the state $x_c(t)$, instead of the bilinear approximated term of the state $x_d(t)$ there exists discrepancy between the digitally redesigned approximated states $x_d(kT)$ and $x_c(kT)$. This is due to the use of approximation via the principle of equivalent areas. When the system of interest in equation (2-1) is unstable, the discrepancy of the state matching between $x_d(kT)$ and $x_c(kT)$ might produce a degradation in the performance of the digitally redesigned system. The lifted state-matching digital redesign method can be employed to develop the lifted digital control law to improve the performance of the digitally redesigned stable/unstable sampled-data systems.

The sampled-data system with a set of lifted fast-rate sampled input $\bar{u}_d(k_f T_f)$ can be represented as

$$\dot{x}_d(t) = Ax_d(t) + B\sum_{k_f=1}^{N} \bar{u}_{dk_f}(k_f T_f), \tag{3-10}$$

where $T_f = T/N$. T is the slow sampling period, T_f is the fast sampling period and N is the sampling ratio during a slow sampling period T. The associated fast-sampled discrete-time system in equation (3-10), with $N = 1$ and $\bar{u}_d(k_f T_f) = u_d(k_f T_f)$, becomes

$$x_d(k_f T_f + T_f) = G_N x_d(k_f T_f) + H_N u_d(k_f T_f), \tag{3-11}$$

where $G_N = e^{AT_f}$ and $H_N = [G_N - I_N]A^{-1}B$.

In addition, the corresponding discrete-time model in equation (3-10) for a slow-sampled system with a lifted fast-sampled input for $kT \leq t < kT + T$ and $kT = k_f T_f$ can be written as

$$x_d(kT + T) = G_N^N x_d(kT) + \bar{H}_N^{(N)} u_d^{(N)}(kT), \tag{3-12}$$

where the lifted system matrix G_N^N becomes $G_N^N = (G_N)^N = e^{AT}$ and the lifted input matrix $\bar{H}_N^{(N)}$ is defined as

$$\begin{aligned} \bar{H}_N^{(N)} &= [\bar{H}_1, \bar{H}_2, \cdots, \bar{H}_{n-1}, \bar{H}_n], \\ &= [G_N^{N-1} H_N, G_N^{N-2} H_N, \cdots, G_N H_N, H_N] \in R^{nxmN}, \end{aligned}$$

and the lifted input vector $\bar{u}_d^{(N)}(kT)$ is defined as

$$\begin{aligned} \bar{u}_d^{(N)}(kT) &= [\bar{u}_{d1}^T(kT), \bar{u}_{d2}^T(kT), \cdots, \bar{u}_{dN}^T(kT)] \\ &= \begin{bmatrix} u_c(kT) \\ u_c(kT + T_f) \\ \vdots \\ u_c(kT + (N-1)T_f) \end{bmatrix} \in R^{nNx1}, \end{aligned}$$

where $\bar{H}_i = G_N^{N-i} H_N$ with $H_N = (G_N - I_N) A^{-1} B$ and $\bar{u}_{d_i}(kT) = u_c(t)$ at $t = kT + (i - 1)T_f$ for $i = 1, 2, \cdots, N$.

The discrete-time system in equation (3-12) can be considered as a multi-input/multi-output (MIMO) discrete-time system and the corresponding lifted state feedback control law for equation (3-12) can be written as

$$\bar{u}_d^{(N)}(kT) = -\bar{K}_d^{(N)} x_d(kT) + \bar{E}_d^{(N)} r(kT), \tag{3-13}$$

where the lifted control gains $\bar{K}_d^{(N)}$ and $\bar{E}_d^{(N)}$ are defined as

$$\bar{K}_d^{(N)} = \begin{bmatrix} K_{d1} \\ K_{d2} \\ \vdots \\ K_{dN} \end{bmatrix} \in R^{mNxn}, \tag{3-14}$$

$$\bar{E}_d^{(N)} = \begin{bmatrix} E_{d1} \\ E_{d2} \\ \vdots \\ E_{dN} \end{bmatrix} \in R^{mNxm}, \tag{3-15}$$

and $r(t)$ is a constant reference input. Substituting equation (3-13) into (3-12) results in the closed-loop digitally redesigned system via N-delay lifting method as shown below,

$$x_d(kT+T) = \left(G_N^N - \bar{H}_N^{(N)} \bar{K}_d^{(N)}\right) x_d(kT) + \bar{H}_N^{(N)} \bar{E}_d^{(N)} r(kT). \tag{3-16}$$

It is desirable to find the digitally redesigned gains $\bar{K}_d^{(N)}$ and $\bar{E}_d^{(N)}$ in equation (3-13) such that the discrete-time states $x_d(kT+T)$ and $x_d(kT)$ in equation (3-16) are exactly matched with the continuous-time states $x_c(kT+T)$ and $x_c(kT)$, in equation (2-7), respectively. Comparing equations (2-7) and (3-16) results in

$$G_c = G_N^N - \bar{H}_N^{(N)} \bar{K}_d^{(N)}, \tag{3-17}$$

$$H_c = \bar{H}_N^{(N)} \bar{E}_d^{(N)}, \tag{3-18}$$

where $G_c \in R^{nxn}, G_N^N \in R^{nxn}, \bar{H}_N^{(N)} \in R^{nxmN}, \bar{K}_d^{(N)} \in R^{mNxn}$ and $\bar{E}_d^{(N)} \in R^{mNxm}$. Approximation methods in Chapter 2 were derived because equations (3-17) and (3-18)

can not be solved easily due to matrix sizes of G_N^N and $\bar{H}_N^{(N)}$ not matching. However, by using the lifting method, the following condition can be achieved and digital gains can be solved. When the dimension $mN \geq n$ and $rank\left(\bar{H}_N^{(N)}\right) = n$, the desired lifted digital gains in equation (3-13) can be solved from equations (3-17) and (3-18) as

$$\bar{K}_d^{(N)} = \left(\bar{H}_N^{(N)}\right)^+ (G_N^N - G_c), \tag{3-19}$$

$$\bar{E}_d^{(N)} = (\bar{H}_N^{(N)})^+ H_c E_c, \tag{3-20}$$

where $(\bar{H}_N^{(N)})^+ = (\bar{H}_N^{(N)})^T [\bar{H}_N^{(N)} (\bar{H}_N^{(N)})^T]^{-1}$. The digital control law in equation (3-13) with digital gains in equations (3-19) and (3-20) is the exact state-matching digital redesign method.

CHAPTER 4 - MULTI-RATE DIGITAL REDESIGN TECHNIQUE

In this section, two topics are discussed. First, the ideal state reconstructor and second the methods above will be expanded to include a system with both analog feedback and cascade controllers.

4.1 Ideal state reconstructing algorithm

In order to use state feedback control to achieve the desired output characteristics, it is required to have the states available to connect to the controller. However, states are not readily available. As depicted in Figure 2-1, in the multi-rate cascaded and output feedback digital control structures, only the input-output signals of $G_1(s)$ are available. In order to avoid the complexity of building state observers [22,25], an ideal state reconstructing algorithm [17] is employed to generate the real discrete-time states of the systems.

Rewriting the discrete-time model of equation (2-1) as in equation (2-12) without the subscripts results as

$$x(kT+T) = Gx_d(kT) + Hu_d(kT), \tag{4-1}$$

$$y(kT) = Cx_d(kT), \tag{4-2}$$

where $G = e^{AT}$, $H = (G - I_n)A^{-1}B$, for a non-singular matrix A. When the matrix A is a singular matrix, the matrix H can be evaluated as $H = \sum_{i=1}^{\infty} \frac{T}{i!}(AT)^{i-1}B$. In order to

reconstruct the state in equations (4-1) and (4-2), a fast-rate sampler is employed $T_f = T/N$, where $N > 1$ is an integer. Slow-rate digital model (G, H, C) can be expressed with fast-rate model (G_N, H_N, C) as

$$G_N = e^{AT_f} = e^{AT/N} = G^{1/N} \triangleq \sqrt[N]{G} \implies (G_N)^{-i} \triangleq \left(\sqrt[N]{G}\right)^{-i}, \tag{4-3}$$

$$H_N = [G_N - I_n]A^{-1}B \Rightarrow (H_N)^{-i} \triangleq \left[(G_N)^{-i} - I_n\right]A^{-1}B, \tag{4-4}$$

where $\sqrt[N]{G}$ is the Nth root of the matrix G [24]. After the zero order hold, $u(kT)$ is a piecewise constant, therefore, the following will be true,

$$u\left(kT - iT_f\right) = u(kT - T), \tag{4-5}$$

for $0 < i \leq N$.

If the matrix G has eigenvalues on the negative real axis for an assigned sampling period T, the unique N_ith root of the matrix G cannot be determined. In this case, a bisection search method can be applied to select a reduced sampling period so that the matrix G would not have eigenvalues on the negative real axis.

Converting equations (4-1) and (4-2) by using the sampling period T_f an equivalent fast-rate sampling digital model is obtained as

$$x\left(\hat{k}T_f + T_f\right) = G_N x\left(\hat{k}T_f\right) + H_N u(\hat{k}T_f), \tag{4-6}$$

$$y\left(\hat{k}T_f\right) = Cx\left(\hat{k}T_f\right), \tag{4-7}$$

Let $\hat{k}T_f = kT$, then equations (4-6) becomes

$$x(kT + T_f) = G_N x(kT) + H_N u(kT). \tag{4-8}$$

Only the input and output values of the system are available, in order to calculate the state variables in one period time (T), N previous values of the input and the output values are used. Therefore moving one fast sampling period back in equation (4-8) results in the following equation,

$$x(kT) = G_N x(kT - T_f) + H_N u(kT - T_f), \tag{4-9}$$

where $u(kT - T_f) = u(kT - T)$, which results as

$$x(kT) = G_N x(kT - T_f) + H_N u(kT - T). \tag{4-10}$$

Previous discrete-time state value is obtained by moving $x(kT - T_f)$ to the right hand side of equation (4-10) with present input and output data. Therefore,

$$x(kT - T_f) = (G_N)^{-1} x(kT) - (G_N)^{-1} H_N u(kT - T)$$

$$x(kT - T_f) = (G_N)^{-1} x(kT) + (H_N)^{-1} u(kT - T)$$

$$x(kT - 2T_f) = (G_N)^{-2} x(kT) + (H_N)^{-2} u(kT - T)$$

$$\vdots$$

$$x(kT - iT_f) = (G_N)^{-i} x(kT) + (H_N)^{-i} u(kT - T),$$

for $i = 1, 2, \cdots, N_f - 1$. Recalling every input and output value at every fast sampling period (T_f) in one slow sampling period (T) the exact state value can be calculated as

$$y = \begin{bmatrix} y(kT) \\ y(kT - T_f) \\ y(kT - 2T_f) \\ \vdots \\ y(kT - (N-1)T_f) \end{bmatrix} = C \begin{bmatrix} x(kT) \\ x(kT - T_f) \\ x(kT - 2T_f) \\ \vdots \\ x(kT - (N-1)T_f) \end{bmatrix}$$

$$= C \begin{bmatrix} x(kT) \\ (G_N)^{-1}x(kT) + (H_N)^{-1}u(kT - T) \\ (G_N)^{-2}x(kT) + (H_N)^{-2}u(kT - T) \\ \vdots \\ (G_N)^{-(N-1)}x(kT) + (H_N)^{-(N-1)}u(kT - T) \end{bmatrix}.$$

Rewriting the equation above as

$$y = Dx(kT) + Eu(kT - T), \tag{4-11}$$

where

$$D = \begin{bmatrix} C \\ C(G_N)^{-1} \\ C(G_N)^{-2} \\ \vdots \\ C(G_N)^{-(N-1)} \end{bmatrix}, E = \begin{bmatrix} 0_{pxm} \\ C(H_N)^{-1} \\ C(H_N)^{-1} \\ \vdots \\ C(H_N)^{-(N-1)} \end{bmatrix}.$$

Moving $x(kT)$ to the left hand side of equation (4-11), then the following equation,

$$Dx(kT) = y - Eu(kT - T), \tag{4-12}$$

is obtained. Since the $rank(D) = n$, the left-side pseudo inverse of the "D" vector is evaluated and $x(kT)$ is calculated as

$$x(kT) = (D^T D)^{-1} D^T [y - Eu(kT - T)]. \tag{4-13}$$

4.2 New multi-rate digital control law redesign

Digital redesign of the control law for the multi-rate sampled-data control system is shown in Figure 2-2. The following continuous-time state equations are obtained and using the following equations the analogy between simple feedback, cascaded gain and state-feedback and state-cascaded gain are observed.

$$\begin{aligned}
\dot{x}_{c1}(t) &= A_1 x_{c1}(t) + B_1 u_{c1}(t) = A_1 x_{c1}(t) + B_1 [C_2 x_{c2}(t) + D_2 u_{c2}(t)] \\
&= A_1 x_{c1}(t) + B_1 \big[C_2 x_{c2}(t) + D_2 [E_c r(t) - y_{c3}(t)]\big] \\
&= A_1 x_{c1}(t) + B_1 C_2 x_{c2}(t) + B_1 D_2 E_c r(t) - B_1 D_2 [C_3 x_{c3}(t) + D_3 u_{c3}(t)] \\
&= A_1 x_{c1}(t) + B_1 C_2 x_{c2}(t) + B_1 D_2 E_c r(t) - B_1 D_2 C_3 x_{c3}(t) \\
&\quad - B_1 D_2 D_3 C_1 x_{c1}(t),
\end{aligned} \tag{4-14}$$

$$\begin{aligned}
\dot{x}_{c2}(t) &= A_2 x_{c2}(t) + B_2 u_{c2}(t) = A_2 x_{c2}(t) + B_2 [E_c r(t) - y_{c3}(t)] \\
&= A_2 x_{c2}(t) + B_2 E_c r(t) - B_2 C_3 x_{c3}(t) - B_2 D_3 u_{c3}(t) \\
&= A_2 x_{c2}(t) + B_2 E_c r(t) - B_2 C_3 x_{c3}(t) - B_2 D_3 C_1 x_{c1}(t),
\end{aligned} \tag{4-15}$$

$$\begin{aligned}
\dot{x}_{c3}(t) &= A_3 x_{c3}(t) + B_3 u_{c3}(t) \\
&= A_3 x_{c3}(t) + B_3 C_1 x_{c1}(t),
\end{aligned} \tag{4-16}$$

where $x_{c1}(t) \in R^{n_1 x1}$, $x_{c2}(t) \in R^{n_2 x1}$, $x_{c3}(t) \in R^{n_3 x1}$ are the state variables, $u_{c1}(t) \in R^{m_1 x1}$, $u_{c2}(t) \in R^{m_2 x1}$, $u_{c3}(t) \in R^{m_3 x1}$ are the input vectors, and $y_{c1}(t) \in R^{p_1 x1}$, $y_{c2}(t) \in R^{p_2 x1}$, $y_{c3}(t) \in R^{p_3 x1}$ are the output vectors. Also, as mentioned in chapter 2, D_1 is assumed as zero.

The extended overall closed-loop state equation for a single-rate sampled-data control system becomes

$$\begin{aligned}\dot{x}_{ec}(t) &= (A_e - B_e K_{ec})x_{ec}(t) + B_e E_{ec} r(t) \\ &= A_{ec}x_{ec}(t) + B_{ec}u_{ec}(t),\end{aligned} \tag{4-17}$$

$$u_{ec} = -K_{ec}x_{ec}(t) + E_{ec}r(t), \tag{4-18}$$

where $A_{ec} = A_e - B_e K_{ec}$.

Equations (4-14), (4-15) and (4-16) combined together can be represented as follows

$$\dot{x}_{ec}(t) = \begin{bmatrix} A_1 - B_1 D_2 D_3 C_1 & B_1 C_2 & -B_1 D_2 C_3 \\ -B_2 D_3 C_1 & A_2 & -B_2 C_3 \\ B_3 C_1 & 0 & A_3 \end{bmatrix} \begin{bmatrix} x_{c1}(t) \\ x_{c2}(t) \\ x_{c3}(t) \end{bmatrix} + \begin{bmatrix} B_1 D_2 \\ B_2 \\ 0 \end{bmatrix} E_c r(t), \tag{4-19}$$

where $x_{ec}^T(t) = [x_{c1}^T(t) \;\; x_{c2}^T(t) \;\; x_{c3}^T(t)]$. Equation (4-18) can be also represented as shown below

$$\begin{aligned}\dot{x_c}(t) = &\left(\begin{bmatrix} A_1 & 0 & 0 \\ 0 & A_2 & 0 \\ 0 & 0 & A_3 \end{bmatrix} - \begin{bmatrix} B_1 & 0 & 0 \\ 0 & B_2 & 0 \\ 0 & 0 & B_3 \end{bmatrix} \begin{bmatrix} D_2 D_3 C_1 & -C_2 & D_2 C_3 \\ D_3 C_1 & 0 & C_3 \\ -C_1 & 0 & 0 \end{bmatrix} \right) \begin{bmatrix} x_{c1}(t) \\ x_{c2}(t) \\ x_{c3}(t) \end{bmatrix} \\ &+ \begin{bmatrix} B_1 & 0 & 0 \\ 0 & B_2 & 0 \\ 0 & 0 & B_3 \end{bmatrix} \begin{bmatrix} D_2 E_c \\ E_c \\ 0 \end{bmatrix} r(t),\end{aligned}$$

where

$$A_e = \begin{bmatrix} A_1 & 0 & 0 \\ 0 & A_2 & 0 \\ 0 & 0 & A_3 \end{bmatrix}, B_e = \begin{bmatrix} B_1 & 0 & 0 \\ 0 & B_2 & 0 \\ 0 & 0 & B_3 \end{bmatrix}, x_{ec} = \begin{bmatrix} x_{c1}(t) \\ x_{c2}(t) \\ x_{c3}(t) \end{bmatrix}, u_{ec} = \begin{bmatrix} u_{c1}(t) \\ u_{c2}(t) \\ u_{c3}(t) \end{bmatrix},$$

$$K_{ec} = \begin{bmatrix} D_2 D_3 C_1 & -C_2 & D_2 C_3 \\ D_3 C_1 & 0 & C_3 \\ -C_1 & 0 & 0 \end{bmatrix} \text{ and } E_{ec} = \begin{bmatrix} D_2 E_c \\ E_c \\ 0 \end{bmatrix}.$$

Since the equivalent continuous-time controller gains K_{ec} and E_{ec} can be calculated from cascaded and output feedback subsystems, the corresponding digital controller gains can be determined using the transformations methods described in Chapter 2. The following equations correspond to the equivalent digital controller gains using the Chebyshev bilinear transform method described in section 2.2

$$K_{ed} = \frac{1}{2}\left(I_{m_1+m_2+m_3} + K_{ec}H_e\right)^{-1} K_{ec}(I_{n_1+n_2+n_3} + G_e), \tag{4-20}$$

$$E_{ed} = \left(I_{m_1+m_2+m_3} + K_{ec}H_e\right)^{-1} E_{ec}, \tag{4-21}$$

where $G_e = e^{A_e T}, H_e = (G_e - I_{n_1+n_2+n_3}){A_e}^{-1}B_e$. The respective state dimensions of $G_1(s)$, $G_2(s)$ and $G_3(s)$ are n_1, n_2 and n_3, respectively. Additionally, m_1, m_2 and m_3 are the respective input numbers of $G_1(s)$, $G_2(s)$ and $G_3(s)$. The digital controller gains using the new improved digital control law are

$$K_{ed} = K_{ec}(A_{ec}T)^{-1}\left(G_{ec} - I_{n_1+n_2+n_3}\right), \tag{4-22}$$

$$E_{ed} = \left[I_{m_1+m_2+m_3} + (K_{ec} - K_{ed})A_{ec}^{-1}B_e\right]E_{ec}, \tag{4-23}$$

where $G_{ec} = e^{A_{ec}T}$.

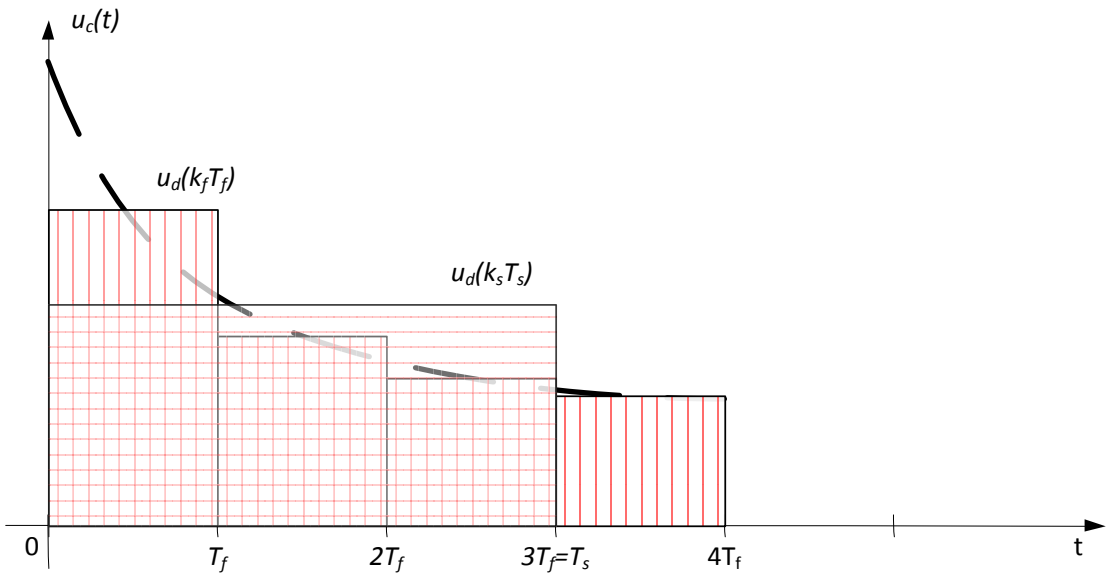

Figure 4-1. Equivalent of multi-rate digital control ($T_s=3T_f$)

In Figure 4-1, various controllers are drawn to show the equivalence of these controllers. Based upon the Chebyshev quadrature method described in chapter 2.2 and the equivalent area concept in Remark 1, the area under $u_c(t)$ for one sampling period T_s, closely matches those of the curves under $u_d(k_fT_f)$ and $u_d(k_sT_s)$ for the sampling period T_s. Hence, the state responses of the system excited by a continuous-time input $u_c(t)$ in Figure 4-1, closely match those of the same system excited by the equivalent fast-rate discrete-time controller $u_d(k_fT_f)$, as well as the equivalent slow-rate discrete-time controller $u_d(k_sT_s)$ in Figure 4-1. As a result, for multi-rate sampling control structures, the desirable multi-rate digitally redesigned control law can be obtained by the combinations of the fast-rate and slow-rate discrete-time controllers.

In this research, multi-rate digital redesign is not calculated simultaneously, for the mathematical analysis of the multi-rate feedback system becomes very complex, even for systems where the ratio of the slow sampling rate to fast sampling rate ($T_{slow}/T_{fast} \geq$

2) is more than two. Therefore the digital controllers are calculated separately for different sampling periods and then then the derived digital controlled systems are merged together.

So considering the different sampling control structures, the multi-rate digital control law redesign steps are described as follows:

1. Compute the single fast-rate sampling digital control law (K_{edf}, E_{edf}) and the single slow-rate sampling digital control law (K_{eds}, E_{eds}) and their corresponding discrete-time states ($x_{edf}(k_fT_f)$, $x_{eds}(k_sT_s)$) for continuous-time closed-loop system in equation (4-17) using equations (4-20) and (4-21), respectively.

$$x_{edf}(k_fT_f) = \begin{bmatrix} x_{d1}(k_fT_f) \\ x_{d2}(k_fT_f) \\ x_{d3}(k_fT_f) \end{bmatrix}, x_{eds}(k_sT_s) = \begin{bmatrix} x_{d1}(k_sT_s) \\ x_{d2}(k_sT_s) \\ x_{d3}(k_sT_s) \end{bmatrix},$$

$$K_{edf} = \begin{bmatrix} K_{d11f} & K_{d12f} & K_{d13f} \\ K_{d21f} & K_{d22f} & K_{d23f} \\ K_{d31f} & K_{d32f} & K_{d33f} \end{bmatrix}, K_{eds} = \begin{bmatrix} K_{d11s} & K_{d12s} & K_{d13s} \\ K_{d21s} & K_{d22s} & K_{d23s} \\ K_{d31s} & K_{d32s} & K_{d33s} \end{bmatrix},$$

$$E_{edf} = \begin{bmatrix} E_{d1f} \\ E_{d2f} \\ E_{d3f} \end{bmatrix}, E_{eds} = \begin{bmatrix} E_{d1s} \\ E_{d2s} \\ E_{d3s} \end{bmatrix}.$$

2. Combine the gains of the fast-rate sampling control law and the slow-rate sampling control law according to the different multi-rate sampling control structures employed in the closed-loop system.

a. The mixed gains (denoted as K_{edfs} and E_{edfs}) of the fast-rate sampling cascaded controller and slow-rate sampling output feedback controller are

$$K_{edfs} = \begin{bmatrix} K_{d11f} & K_{d12f} & K_{d13f} \\ K_{d21f} & K_{d22f} & K_{d23f} \\ K_{d31s} & K_{d32s} & K_{d33s} \end{bmatrix}, \qquad E_{edfs} = \begin{bmatrix} E_{d1f} \\ E_{d2f} \\ E_{d3s} \end{bmatrix}.$$

Also, the equations corresponding to (2-10) for the digital controller gains above become the following,

$$u_{d1f}(kT) = K_{d11f}x_{d1f}(kT) + K_{d12f}x_{d2f}(kT) + K_{d13f}x_{d3f}(kT) + E_{d11f}r(kT), \quad (4\text{-}24)$$

$$u_{d2f}(kT) = K_{d21f}x_{d1f}(kT) + K_{d22f}x_{d2f}(kT) + K_{d23f}x_{d3f}(kT) + E_{d21f}r(kT), \quad (4\text{-}25)$$

$$u_{d3s}(kT) = K_{d31s}x_{d1s}(kT) + K_{d32s}x_{d2s}(kT) + K_{d33s}x_{d3s}(kT) + E_{d31s}r(kT), \quad (4\text{-}26)$$

where subscripts 1, 2 and 3 correspond to plant, cascaded system and the dynamic output feedback system.

b. The mixed gains (denoted as K_{edsf} and E_{edsf}) of the slow-rate sampling cascaded controller and fast-rate sampling output feedback controller are

$$K_{edsf} = \begin{bmatrix} K_{d11s} & K_{d12s} & K_{d13s} \\ K_{d21s} & K_{d22s} & K_{d23s} \\ K_{d31f} & K_{d32f} & K_{d33f} \end{bmatrix}, \qquad E_{edsf} = \begin{bmatrix} E_{d1s} \\ E_{d2s} \\ E_{d3f} \end{bmatrix}.$$

Also, the equations corresponding to (2-10) for the digital controller gains above become the following,

$$u_{d1s}(kT) = K_{d11s}x_{d1s}(kT) + K_{d12s}x_{d2s}(kT) + K_{d13s}x_{d3s}(kT) + E_{d11s}r(kT), \quad (4\text{-}27)$$

$$u_{d2s}(kT) = K_{d21s}x_{d1s}(kT) + K_{d22s}x_{d2s}(kT) + K_{d23s}x_{d3s}(kT) + E_{d21s}r(kT), \quad (4\text{-}28)$$

$$u_{d3f}(kT) = K_{d31f}x_{d1f}(kT) + K_{d32f}x_{d2f}(kT) + K_{d33f}x_{d3f}(kT) + E_{d31f}r(kT), \quad (4\text{-}29)$$

where subscripts 1, 2 and 3 correspond to plant, cascaded system and the dynamic output feedback system.

The completed multi-rate digitally redesigned sampled-data system is shown in Figure 4-2. In the multi-rate digital control system for case 1, where Γ is the final-value scaling factor of the unit-step response of the closed-loop system, SR is the ideal state reconstructor.

For the improved digital redesign method, the same procedure is carried out that is described above for the digital gains K_{ed} and E_{ed} obtained in equations (4-22) and (4-23). For the combination of the gains of the fast-rate and slow-rate sampling controllers, the final value of the unit-step response of the digitally controlled plant $G_1(s)$ may deviate from that of the original continuous-time system, so a final-value scaling factor Γ can be used to compensate the steady state value of the digitally redesigned closed-loop system. Γ is calculated as $\Gamma = y_{c1}(\infty)/y_{d1}(\infty)$, where $y_{c1}(\infty)$ is the steady state value of $y_{c1}(t)$ in Figure 2-1, $y_{d1}(\infty)$ is the steady state value of $y_{d1}(t)$ in Figure 4-2, which is the output value of $G_1(s)$ under the digital control law $u_{d1}(t)$.

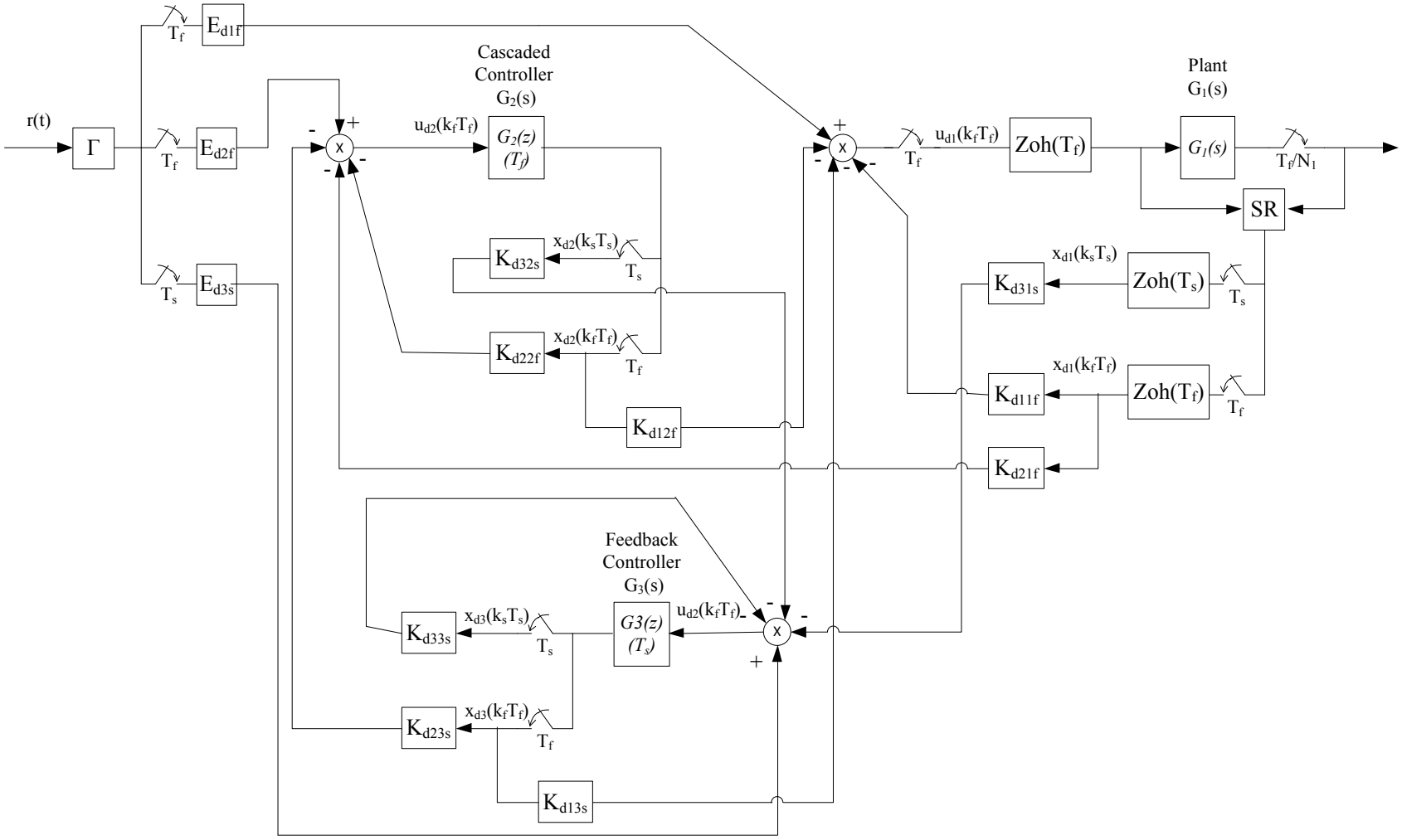

Figure 4-2. Multi-rate digital control system

CHAPTER 5 - ILLUSTRATIVE EXAMPLES

5.1 Example 1

In this example, a liquid level control system [7] with the cascaded and output feedback controllers is described by transfer functions of

$$G_1(s) = \frac{3.15}{30s + 1}$$

$$G_2(s) = \frac{10}{\mathrm{s} + 1}$$

$$G_3(s) = \frac{8.71}{s^2 + 3s + 9}$$

subsystems. Using the digital redesign steps described in Chapter 4 with the fast-rate sampling period, $T_f = 0.2s$ in the cascaded controller $G_2(s)$ and the slow-rate sampling period, $T_s = 0.6s$ in the output feedback controller $G_3(s)$, the digital control law of the improved digital redesign method are

$$K_{edf} = \begin{bmatrix} 0.0026 & -9.0624 & 7.9359 & 0.4699 \\ 0.0052 & 0.0026 & 8.2640 & 0.6996 \\ -0.1046 & -0.0981 & 0.0570 & 0.0026 \end{bmatrix}, E_{edf} = \begin{bmatrix} 0.9365 \\ 0.9999 \\ 0.0067 \end{bmatrix}, (T_f = 0.2s)$$

$$K_{eds} = \begin{bmatrix} 0.0479 & -7.4626 & 17.4286 & 2.6035 \\ 0.0320 & 0.0479 & 5.8996 & 1.2222 \\ -0.1033 & -0.2580 & 0.4153 & 0.0479 \end{bmatrix}, E_{eds} = \begin{bmatrix} 2.4740 \\ 0.9937 \\ 0.0542 \end{bmatrix}, (T_s = 0.6s)$$

as above. The digital control law of the Chebyshev bilinear method is

$$K_{edf} = \begin{bmatrix} 0.0060 & -9.0855 & 7.4011 & 0.5693 \\ 0.0066 & 0.0060 & 8.1412 & 0.6262 \\ -0.1046 & -0.0951 & 0.0775 & 0.0060 \end{bmatrix}, E_{edf} = \begin{bmatrix} 1.8096 \\ 0.9953 \\ 0.0379 \end{bmatrix}, (T_f = 0.2)$$

$$K_{eds} = \begin{bmatrix} 0.0680 & -7.5354 & 13.8048 & 2.1797 \\ 0.0295 & 0.0680 & 5.9821 & 0.9445 \\ -0.1018 & -0.2350 & 0.4305 & 0.0680 \end{bmatrix}, E_{eds} = \begin{bmatrix} 3.9564 \\ 0.8572 \\ 0.2468 \end{bmatrix}, (T_s = 0.6s)$$

as above. The final scaling factor is Γ = 1.052077 for the Chebyshev bilinear method. For comparison, it is also calculated the unit-step responses of the control laws of the direct bilinear transform method and the single-rate sampling digital control with $T = T_f = 0.2s$. Figure 5-1 shows the simulation results of the unit-step responses of the closed-loop systems. The percentage error of the original continuous-time system vs. the system via the proposed Chebyshev bilinear method is defined as $\frac{\sum_{k=1}^{kf}|y_{org}(kT_f)-y_{ind}(kT_f)|}{\sum_{k=1}^{kf}|y_{org}(kT_f)|}x100$, where the final sampling index k_f = 160, is given by 0.9054%. Similarly, the percentage errors of the original continuous-time system vs. the systems via the improved digital method and the direct bilinear method are 0.3248% and 1.4896%, respectively. It is clear that when the fast-rate sampling used in the cascaded controller and the slow-rate sampling employed in the output feedback controller, the proposed indirect digital method and the Chebyshev bilinear method perform much better than that of the direct bilinear method in both transient and steady state response of the closed-loop system. The performance of the improved digital method is better than that of the Chebyshev bilinear method.

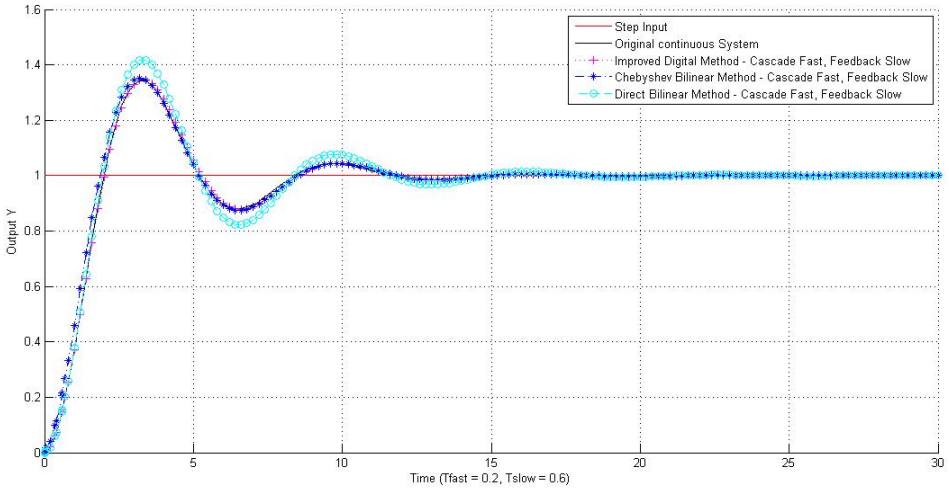

Figure 5-1. Unit-step responses of multi-rate sampled-data system (T_f/T_s)

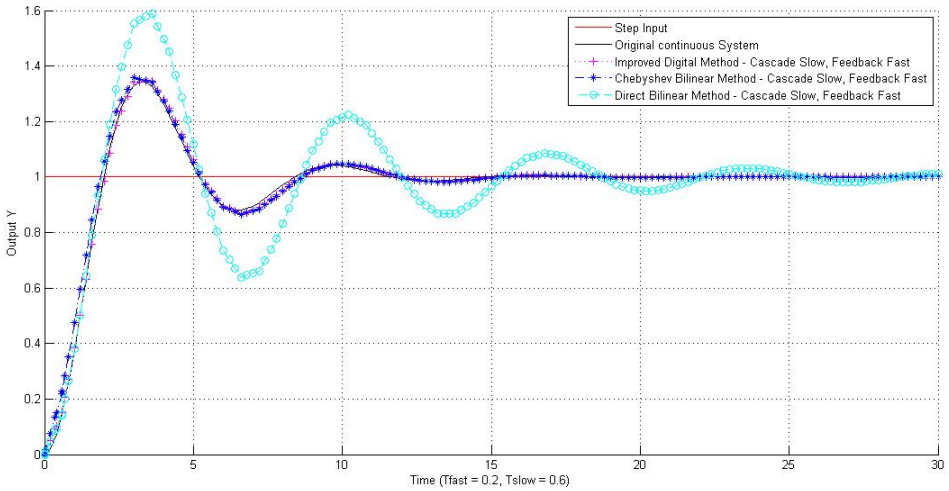

Figure 5-2. Unit-step responses of multi-rate sampled-data system (T_s/T_f)

On the other hand, if we use the fast-rate sampling period $T_f = 0.2s$ in the output feedback controller $G_3(s)$ and the slow-rate sampling period $T_s = 0.6s$ in the cascaded controller $G_2(s)$, the unit-step responses of the closed-loop systems are shown in Figure 5-2. The percentage errors of the original continuous system vs. the systems via the Chebyshev bilinear method, the improved digital method, and the direct bilinear method

for k_f = 160 are 1.2836%, 0.5687%, 7.3357%. Similarly, the performances of the proposed methods are much better than that of the direct bilinear transform method.

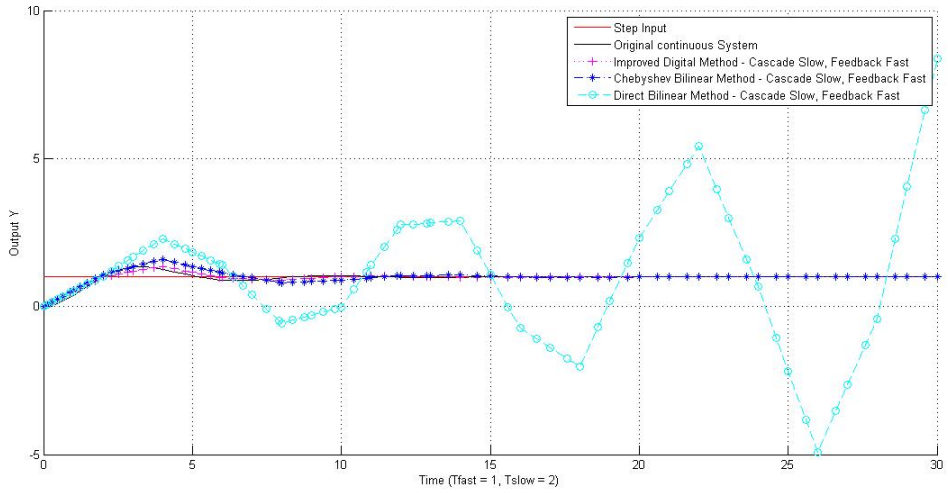

Figure 5-3. Unit-step responses of multi-rate sampled-data system with long time sampling

As mentioned in abstract, although the direct bilinear method is a fairly simple and widely used method, it is an open-loop design which does not take closed-loop stability into account. Sampling periods of the digital redesigned system are changed to $T_f = 1s$ and $T_s = 2s$, as shown in Figure 5-3, and it is obvious that the digitally redesigned system follows the continuous-time output; however, the direct bilinear transformation method is unstable.

5.2 Example 2

In the second example, an electro-mechanical control system structure [3] with subsystems as

$$G_1(s) = \frac{3s + 2.5}{s^2 + 2s + 3},$$

$$G_2(s) = \frac{s + 2}{s + 3},$$

$$G_3(s) = \frac{s^2 + 2s + 1}{s^2 + 4s + 5},$$

specified above. Following the redesign step in Chapter 4 with the fast-rate sampling period $T_f = 0.1s$ in the cascaded controller $G_2(s)$ and the slow-rate sampling period $T_s = 0.3s$ in the output feedback controller $G_3(s)$, the digital control laws of the improved digital redesign method are

$$K_{edf} = \begin{bmatrix} 1.5335 & 2.1219 & 0.7564 & -2.9430 & -1.5102 \\ 1.6182 & 2.2332 & -0.1112 & -3.0951 & -1.5875 \\ -1.8063 & -2.4794 & 0.1192 & -0.4685 & -0.2383 \end{bmatrix},$$

$$E_{edf} = \begin{bmatrix} 0.8393 \\ 0.8808 \\ 0.1276 \end{bmatrix}, (T_f = 0.1s)$$

$$K_{eds} = \begin{bmatrix} 0.5088 & 1.1367 & 0.4877 & -1.7742 & -0.9605 \\ 0.6226 & 1.3271 & -0.1904 & -2.0527 & -1.1072 \\ -0.9424 & -1.8461 & 0.2376 & -0.8962 & -0.4717 \end{bmatrix},$$

$$E_{eds} = \begin{bmatrix} 0.6707 \\ 0.7621 \\ 0.2932 \end{bmatrix}, (T_s = 0.3s)$$

as specified above. The digital control law of the chebyshev bilinear method are

$$K_{edf} = \begin{bmatrix} 1.2818 & 1.7416 & 0.7181 & -2.6741 & -1.3681 \\ 1.4039 & 1.9074 & -0.1659 & -2.9288 & -1.4984 \\ -1.7151 & -2.3303 & 0.2026 & -0.7545 & -0.3860 \end{bmatrix},$$

$$E_{edf} = \begin{bmatrix} 0.7540 \\ 0.8258 \\ 0.2128 \end{bmatrix}, (T_f = 0.1s)$$

$$K_{eds} = \begin{bmatrix} 0.4547 & 0.8076 & 0.5226 & -1.7195 & -0.9124 \\ 0.5733 & 1.0183 & -0.2107 & -2.1681 & -1.1504 \\ -1.0528 & -1.8701 & 0.3869 & -1.2731 & -0.6755 \end{bmatrix},$$

$$E_{eds} = \begin{bmatrix} 0.6009 \\ 0.7577 \\ 0.4449 \end{bmatrix}, (T_s = 0.3s)$$

as above. The final scaling factor is Γ = 0.946063 for the Chebyshev bilinear method. The unit-step responses of the improved digital redesign method, the Chebyshev bilinear method, the direct bilinear transform method and the original continuous-time closed-loop system are presented in Figure 5-4. The percentage errors of the original continuous-time system vs. the system via the Chebyshev bilinear method, improved digital redesign method, and the direct bilinear method for $k_f = 108$ are 1.33%, 0.1795%, 1.8087% respectively. From the simulation results, it is shown that the direct bilinear transform method cannot tract the transient response of the original continuous-time system correctly, while the proposed Chebyshev bilinear and improved digital redesign methods still exhibit acceptable levels of performance.

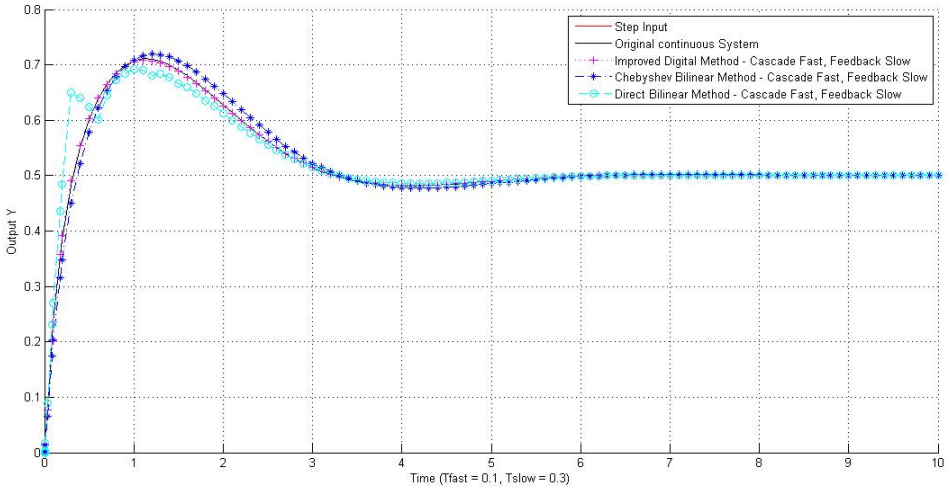

Figure 5-4. Unit-step responses of multi-rate sampled-data system (T_f/T_s)

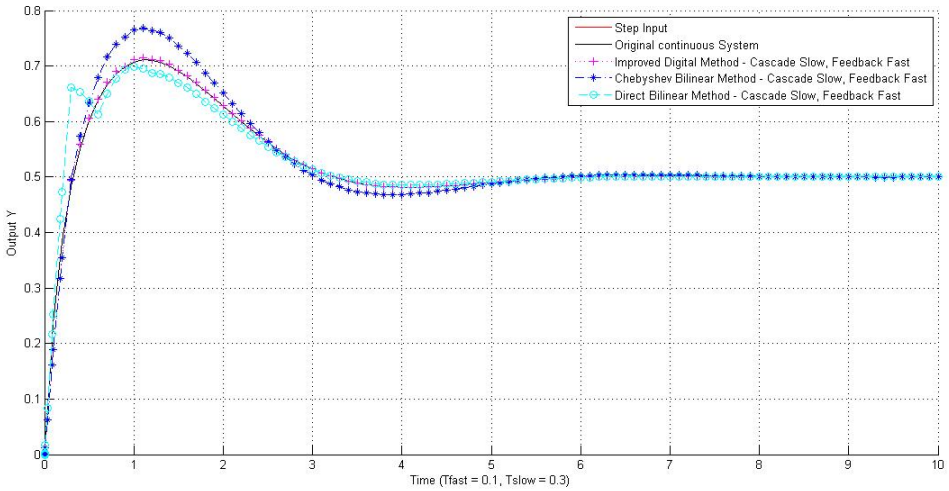

Figure 5-5. Unit-step responses of the multi-rate sampled-data system (T_s/T_f)

If we employ the fast-rate sampling period $T_f = 0.1s$ in the output feedback controller $G_3(s)$ and slow-rate sampling period $T_s = 0.3s$ in the cascaded controller $G_2(s)$, the unit-step responses of the closed-loop systems are shown in Figure 5-5. The percentage errors of the original continuous-time system vs. the systems via the Chebyshev bilinear method, improved digital redesign method, and the direct bilinear

method for k_f = 108 are 2.4270%, 0.4925%, and 1.6902% respectively. The performances of the proposed methods are better than that of the direct bilinear transform method.

5.3 Example 3

In the third example, consider the control system structure with subsystems as

$$G_1(s) = \frac{-s + 2}{s^2 + 2s + 3},$$

$$G_2(s) = \frac{s + 1}{s + 2},$$

$$G_3(s) = \frac{s^2 + 2s + 2}{s^2 + 4s + 5},$$

specified above. Following the redesign step in Chapter 4 with the fast-rate sampling period $T_f = 0.05s$ in the cascaded controller $G_2(s)$ and the slow-rate sampling period $T_s = 0.1s$ in the output feedback controller $G_3(s)$, the digital control laws of the improved digital redesign method are

$$K_{edf} = \begin{bmatrix} 1.9679 & -0.8555 & 0.9734 & -2.7544 & -1.8752 \\ 2.0166 & -0.8776 & 0.0222 & -2.8241 & -1.9223 \\ -2.1163 & 0.9223 & 0.0229 & 0.0662 & 0.0447 \end{bmatrix},$$

$$E_{edf} = \begin{bmatrix} 0.9980 \\ 1.0226 \\ -0.0233 \end{bmatrix}, (T_f = 0.05s)$$

$$K_{eds} = \begin{bmatrix} 1.9230 & -0.7219 & 0.9442 & -2.5186 & -1.7517 \\ 2.0174 & -0.7611 & 0.0392 & -2.6479 & -1.8404 \\ -2.2156 & 0.8434 & -0.0419 & 0.1160 & 0.0796 \end{bmatrix},$$

$$E_{eds} = \begin{bmatrix} 0.9924 \\ 1.0405 \\ -0.0434 \end{bmatrix}, (T_s = 0.1s)$$

as specified above. The digital control law of the Chebyshev bilinear method are

$$K_{edf} = \begin{bmatrix} 1.8564 & -0.8108 & 0.9910 & -2.7400 & -1.8641 \\ 1.9492 & -0.8514 & 0.0405 & -2.8770 & -1.9573 \\ -2.1516 & 0.9398 & -0.0448 & 0.1237 & 0.0842 \end{bmatrix},$$

$$E_{edf} = \begin{bmatrix} 0.9910 \\ 1.0405 \\ -0.0448 \end{bmatrix}, (T_f = 0.1s)$$

$$K_{eds} = \begin{bmatrix} 1.6896 & -0.6471 & 0.9679 & -2.4747 & -1.7163 \\ 1.8586 & -0.7118 & 0.0647 & -2.7221 & -1.8879 \\ -2.2592 & 0.8652 & -0.0787 & 0.2011 & 0.1395 \end{bmatrix},$$

$$E_{eds} = \begin{bmatrix} 0.9679 \\ 1.0647 \\ -0.0787 \end{bmatrix}, (T_s = 0.3s)$$

as above. The final scaling factor is $\Gamma = 1.03159$ for the Chebyshev bilinear method. The unit-step responses of the improved digital redesign method, the Chebyshev bilinear method, the direct bilinear transform method and the original continuous-time closed-loop system are presented in Figure 5-6. The percentage errors of the original continuous-time system vs. the system via the Chebyshev bilinear method, improved digital redesign method, and the direct bilinear method for $k_f = 126$ are 0.4943%, 0.0366%, and 0.8198% respectively. From the error percentages it is obvious that the proposed Chebyshev bilinear and improved digital redesign methods perform better closed-loop system responses than direct bilinear method and both methods exhibit acceptable levels of performance.

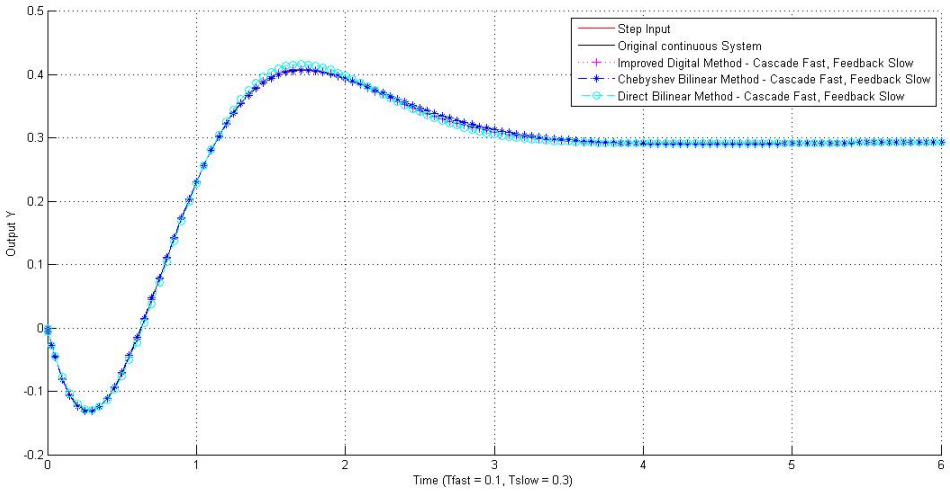

Figure 5-6. Unit-step responses of multi-rate sampled-data system (T_f/T_s)

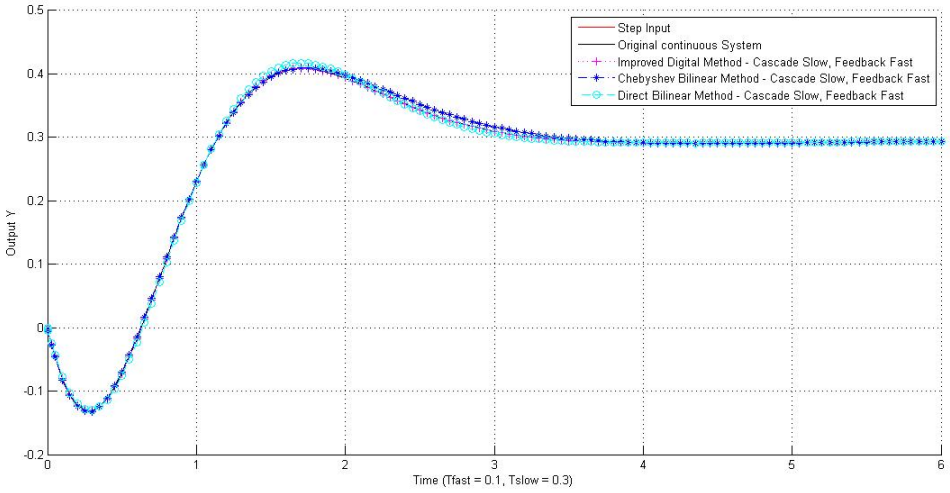

Figure 5-7. Unit-step responses of multi-rate sampled-data system (T_s/T_f)

If we employ the fast-rate sampling period $T_f = 0.05s$ in the output feedback controller $G_3(s)$ and slow-rate sampling period $T_s = 0.1s$ in the cascaded controller $G_2(s)$, the unit-step responses of the closed-loop systems are shown in Figure 5-7. The percentage errors of the original continuous-time system vs. the systems via the Chebyshev bilinear method, improved digital redesign method, and the direct bilinear

method for $k_f = 126$ are 0.9072%, 0.0548%, and 0.8429% respectively. The performance of the improved digital redesign method is better than both of the other methods. Although, direct bilinear transform and Chebyshev bilinear transform perform close results, it is unknown whether the direct bilinear transform will provide closed-loop system response stability.

5.4 Example 4

This example is the same as example 3 except the fast and slow sampling times are changes to $T_f = 0.2s$, and $T_s = 0.4s$, respectively. Following the redesign step in chapter 4, and using the fast-rate sampling period for the cascaded controller $G_2(s)$ and the slow-rate sampling period for the output feedback controller $G_3(s)$, the digital control laws of the improved digital redesign method are

$$K_{edf} = \begin{bmatrix} 1.8031 & -0.4879 & 0.8799 & -2.0804 & -1.5127 \\ 1.9792 & -0.5477 & 0.0598 & -2.3017 & -1.6688 \\ 2.3654 & 0.6801 & -0.0687 & 0.1744 & 0.1235 \end{bmatrix},$$

$$E_{edf} = \begin{bmatrix} 0.9721 \\ 1.0644 \\ -0.0738 \end{bmatrix}, (T_f = 0.2s)$$

$$K_{eds} = \begin{bmatrix} 1.4927 & -0.1450 & 0.7416 & -1.3543 & -1.0877 \\ 1.7890 & -0.2078 & 0.0628 & -1.6714 & -1.3253 \\ -2.4938 & 0.3640 & -0.0852 & 0.1742 & 0.1338 \end{bmatrix},$$

$$E_{eds} = \begin{bmatrix} 0.9082 \\ 1.0748 \\ -0.1000 \end{bmatrix}, (T_s = 0.4s)$$

as specified above. The digital control law using Chebyshev bilinear method are

$$K_{edf} = \begin{bmatrix} 1.3488 & -0.3996 & 0.8999 & -1.9861 & -1.4275 \\ 1.6185 & -0.4796 & 0.0799 & -2.3833 & -1.7130 \\ -2.3706 & 0.7024 & -0.1171 & 0.2584 & 0.1857 \end{bmatrix},$$

$$E_{edf} = \begin{bmatrix} 0.8999 \\ 1.0799 \\ -0.1171 \end{bmatrix}, (T_f = 0.2s)$$

$$K_{eds} = \begin{bmatrix} 0.8108 & -0.1431 & 0.7552 & -1.2838 & -0.9817 \\ 1.1351 & -0.2003 & 0.0572 & -1.7973 & -1.3744 \\ -2.3649 & 0.4173 & -0.1192 & 0.2027 & 0.1550 \end{bmatrix},$$

$$E_{eds} = \begin{bmatrix} 0.7552 \\ 1.0572 \\ -0.1192 \end{bmatrix}, (T_s = 0.4s)$$

as above. The final scaling factor is Γ = 1.12433 for the Chebyshev bilinear method. The unit-step responses of the improved digital redesign method, the Chebyshev bilinear method, the direct bilinear transform method and the original continuous-time closed-loop system are presented in Figure 5-8. The percentage errors of the original continuous-time system vs. the system via the Chebyshev bilinear method, improved digital redesign method, and the direct bilinear method for k_f = 66 are 1.6278%, 0.4604%, and 4.0080% respectively. From the error percentages it is obvious that the proposed Chebyshev bilinear and improved digital redesign methods perform better closed-loop system responses than direct bilinear method and both methods exhibit acceptable levels of performance.

If we employ the fast-rate sampling period $T_f = 0.2s$ in the output feedback controller $G_3(s)$ and slow-rate sampling period $T_s = 0.4s$ in the cascaded controller $G_2(s)$, the unit-step responses of the closed-loop systems are shown in Figure 5-9. The percentage errors of the original continuous-time system vs. the systems via the

Chebyshev bilinear method, improved digital redesign method, and the direct bilinear method for $k_f = 66$ are 4.0414%, 0.8140%, and 8.5239% respectively. The performance of the improved digital redesign method is better than both of the other method. Also, the resulting closed-loop system response of direct bilinear transform method does not reach stability after 6 seconds.

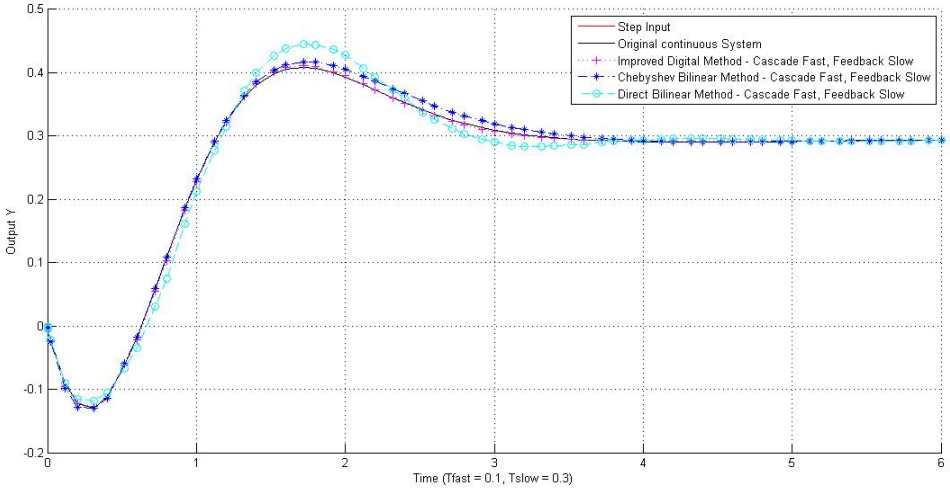

Figure 5-8. Unit-step responses of multi-rate sampled-data system (T_f/T_s)

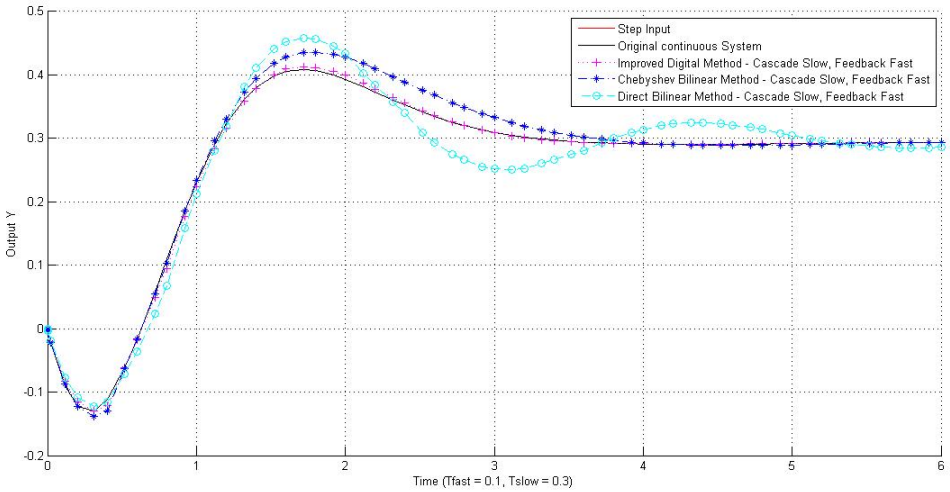

Figure 5-9. Unit-step responses of multi-rate sampled-data system (T_s/T_f)

Comparing examples 3 and 4, it is concluded that the error between the continuous-time system response and redesigned systems is significantly less when the sampling time of the system is decreased.

5.5 Example 5

In the fifth example, consider the unstable control system structure,

$$G_1(s) = \frac{-1}{s^2 + 1.5s - 1}.$$

Continuous-time controller gains are calculated to match the desired continuous-time response. The continuous-time controller gains are

$$K_c = [2 \quad 1], E_c = -1,$$

as shown above. Following the redesign step in chapter 3 with the sampling period $T = 0.2s$ and using N = 2, the digital control laws of the lifted digital redesign method are

$$\bar{K}_d^{(N)} = \begin{bmatrix} 1.9667 & 0.9833 \\ 1.8398 & 0.9199 \end{bmatrix},$$

$$\bar{E}_d^{(N)} = \begin{bmatrix} -0.9667 \\ -0.8398 \end{bmatrix},$$

as specified above. Also, the digital control gains calculated using improved digital redesign method and chebyshev bilinear method are

$$K_{d_{improved}} = [1.9033 \quad 0.9516], E_{d_{improved}} = -0.9033,$$

and

$$K_{d_{chebyshev}} = [1.9048 \quad 0.9524], E_{d_{chebyshev}} = -0.9048,$$

respectively. The unit-step response of the N-delay lifted redesign method and the original continuous-time closed-loop system are presented in Figure 5-8. The percentage errors of the original continuous-time system vs. the system via the N-delay lifting method for k_f = 155 is 9.5695×10^{-6}%, which is an indicates that the redesigned method exactly follows the continuous-time system. Basis of the designed system as explained in Chapter 3 the state matching at every sampling time. The states of the continuous-time system and the N-delay lifted redesigned method are shown in Figure 5-11. As a conclusion it is concluded that using the N-delay lifting method the state variables are matched at every sampling period and as a result both the continuous-time system response and the digitally redesigned system using N-delay lifting method are the same.

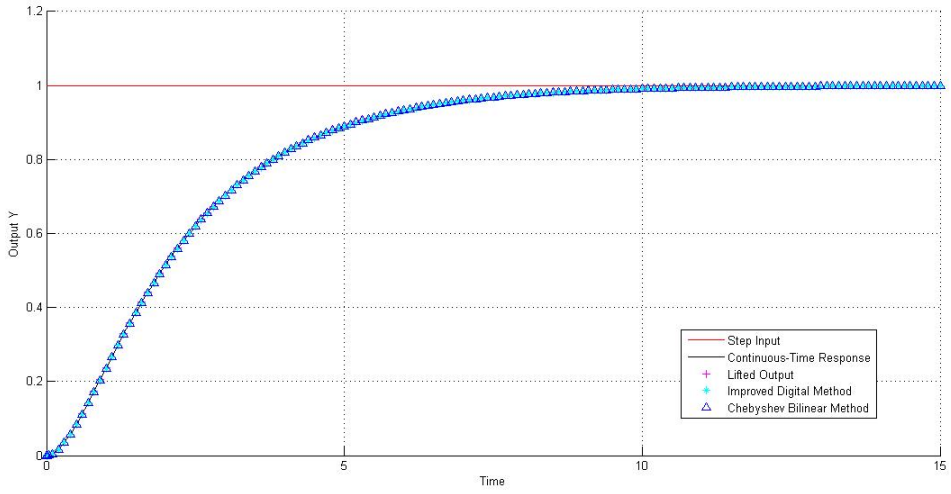

Figure 5-10. Unit-step response of N-delay sampled-data system

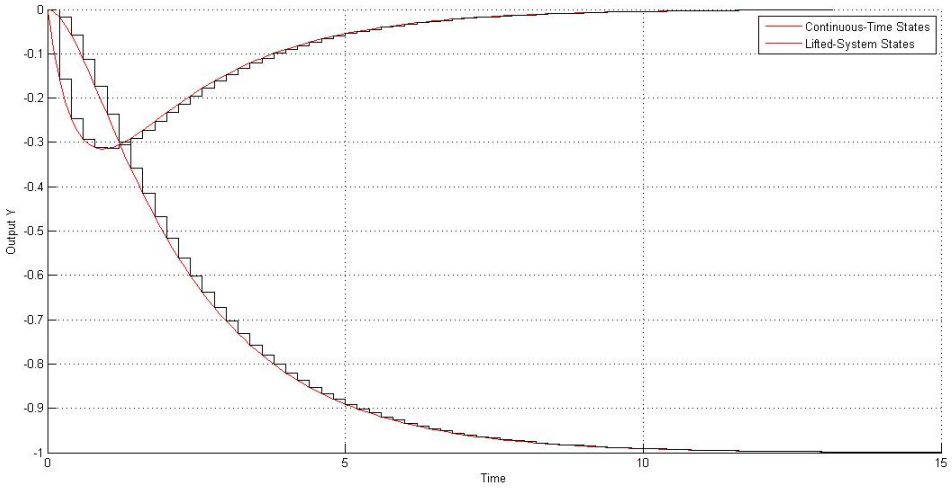

Figure 5-11. State variables for continuous-time system and lifted redesigned system

5.6 Example 6

In the sixth example, consider the multi-input, multi-output system [26] with controllable and observable plant with the following parameters as

$$A = \begin{bmatrix} 0.2 & 1 & 0 \\ 0 & -2 & 1 \\ -2 & -1 & -3 \end{bmatrix}, B = \begin{bmatrix} 2 & 1 \\ 1 & -0.5 \\ 2 & -1 \end{bmatrix}, C = \begin{bmatrix} 1.5 & 0.1 & 0 \\ 0 & 1 & -0.1 \end{bmatrix}, x_{c0} = \begin{bmatrix} 0.7 \\ -0.8 \\ 0.5 \end{bmatrix},$$

and continuous-time controller gains as

$$K_c = \begin{bmatrix} 126.2651 & 61.6655 & -4.6711 \\ 81.0979 & -75.8646 & 6.8861 \end{bmatrix},$$

$$E_c = \begin{bmatrix} 84.0743 & 54.1265 \\ 54.1427 & -84.0603 \end{bmatrix},$$

shown above. Following the redesign steps in chapter 3 with the sampling period T = 0.05s and using N = 2, the digital control laws of the lifted digital redesign method are

$$\bar{K}_d^{(N)} = \begin{bmatrix} 14.0380 & 26.3297 & -1.8816 \\ 8.5621 & -23.5760 & 1.2585 \\ -3.9272 & -4.8879 & 1.0102 \\ 11.0288 & -19.3408 & 0.8653 \end{bmatrix},$$

$$\bar{E}_d^{(N)} = \begin{bmatrix} 9.2574 & 26.2916 \\ 5.7585 & -26.8991 \\ -2.6862 & -3.7890 \\ 7.3984 & -22.8233 \end{bmatrix},$$

as specified above. Also, the digital control gains calculated using improved digital redesign method and Chebyshev bilinear method are

$$K_{d_{improved}} = \begin{bmatrix} 5.0635 & 10.7161 & -0.4352 \\ 9.7912 & -21.4820 & 1.0642 \end{bmatrix}, E_{d_{improved}} = \begin{bmatrix} 3.2910 & 11.2460 \\ 6.5756 & -24.8846 \end{bmatrix},$$

and

$$K_{d_{chebyshev}} = \begin{bmatrix} 10.4226 & 15.1798 & -0.8488 \\ 14.4545 & -28.7176 & 1.8267 \end{bmatrix},$$

$$E_{d_{chebyshev}} = \begin{bmatrix} 6.8643 & 15.3484 \\ 9.6827 & -32.4228 \end{bmatrix}$$

respectively. In this example the output is designed to track the reference input signals, which are sin(t) and cos(t), which are shown in Figure 5-12. The output responses of the N-delay lifted redesign method and the original continuous-time closed-loop system are presented in Figures 5-13 and 5-14. Also, the reference input sin(t) is replaced with a step input and the output still follows the reference input as seen in Figure 5-15. From the figures it is seen that digitally redesigned outputs follow the input references.

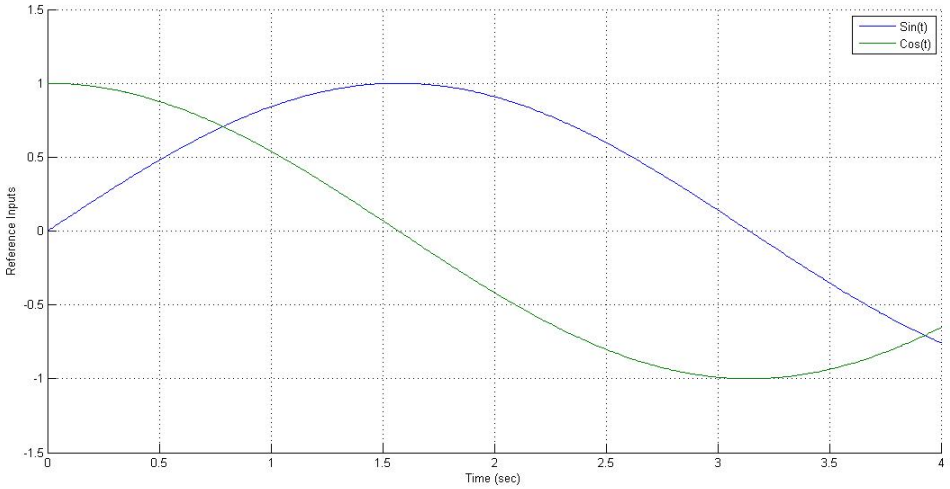

Figure 5-12. Reference inputs

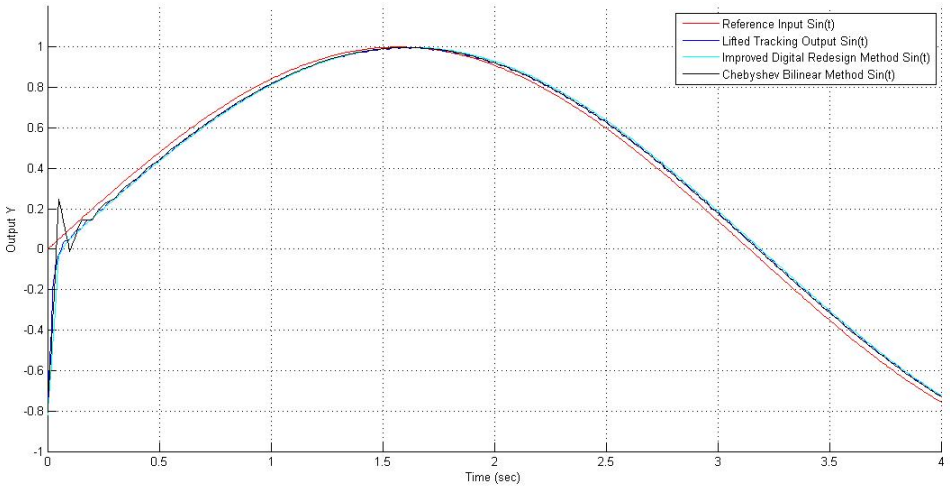

Figure 5-13. Reference input sin(t) and digitally redesigned lifted output

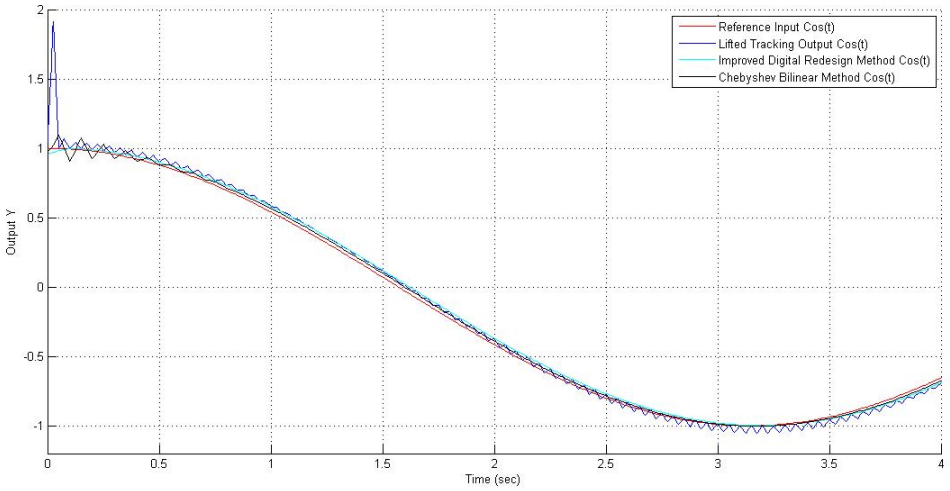

Figure 5-14. Reference input cos(t) and digitally redesigned lifted output

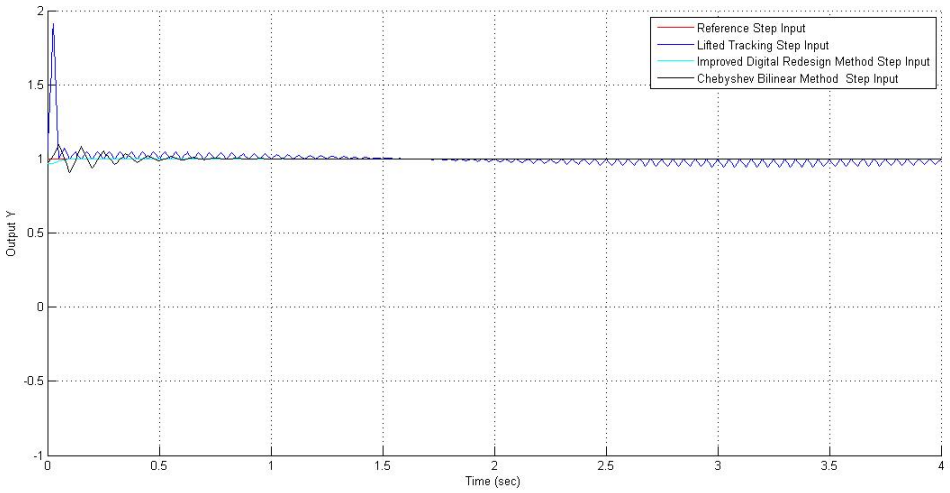

Figure 5-15. Reference input step input and digitally redesigned lifted output

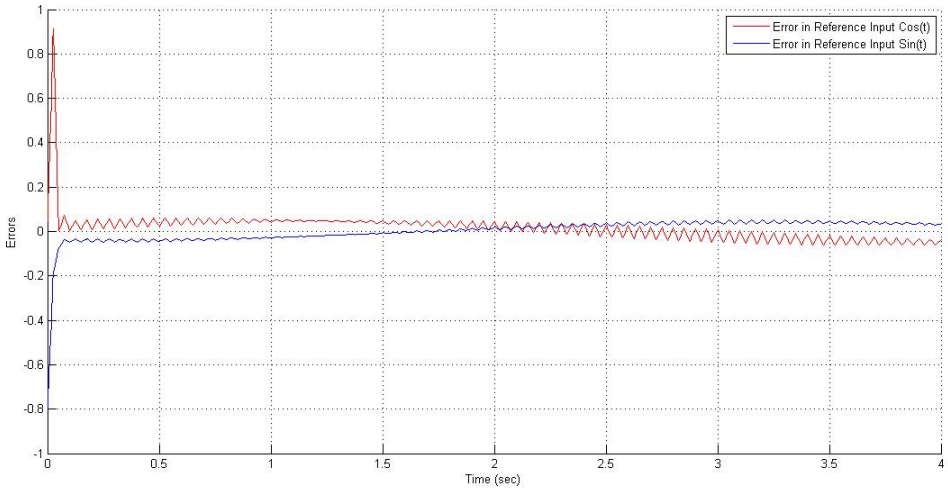

Figure 5-16. Error of digitally redesigned system outputs

CHAPTER 6 - SUMMARY AND CONCLUSIONS

6.1 Summary

The use of multi-rate redesign, N-delay lifting methods has become popular in today's world and has been widely used in several engineering problems. This study presents new approximation methods derived using the Chebyshev bilinear redesign method, the improved digital redesign method for estimating the dynamic output feedback and cascaded controller gains K_d, E_d values, respectively. To implement the redesigned digital state feedback control law, an ideal state reconstructing algorithm is utilized to obtain discrete-time states of the original continuous-time closed-loop system. The approximation methods are further expanded to include systems as cascaded and feedback gains to calculate K_d and E_d matrices. Further research is conducted using the N-delay lifting method to calculate the exact K_d and E_d values. For this purpose, different continuous-time systems (stable/unstable) are simulated using Matlab/Simulink, which resulted in acceptable results in approximation methods and exact output responses for N-delay lifting method. The results using both the approximation and exact methods are compared with widely used more simple methods to indicate the difference between all redesigned systems. The simulated systems are examples that are previously used in books and papers, so that the simulated system is based on real-life problems. After a significant amount of simulations were conducted to accurately model the continuous-time systems and the digital redesigned systems, result of these examples are presented and several conclusions were drawn from this study.

6.2 Conclusions

The study resulted in the following conclusions:

1) Using the Chebyshev bilinear method and the improved digital redesign method, the gains of the digital controllers for a multi-rate sampled-data control system are determined, which ensures the states of the closed-loop hybrid control system closely matching those of the original continuous-time control system.
2) Using the N-delay lifting method, the gains of the digital controllers for a control system are determined, which results in the states of the closed-loop hybrid control system to exactly match those of the original continuous-time control system.
3) The output error percentages of different digital redesign methods are compared, and as expected the lifting method results in almost zero percent error, while Chebyshev bilinear and improved digital redesign indicate between 0.2-4 percent errors which are within acceptable limits. All of the digital redesign methods exhibit a better performance than widely used direct bilinear method, which results in error percentages between 8-17 percent.
4) Proposed multi-rate digital redesign method allows the development of inexpensive an high performance digital controllers for effective hybrid control of continuous-time systems.

5) The simulation results that the developed methods exhibit better output-tracking performance than that of widely used traditional direct bilinear transform method.

6.3 Future Research

Scope of this work was limited to systems with no input delays. The following is a list of ideas for possible future work:

a) Systems with input-time delays could be in developed.

b) Time delay while reconstructing digital states could be examined.

c) The gains for muti-rate sampled-data using N-delay lifting method could be investigated.

d) Research on multi-rate redesign on non-linears systems could be performed.

REFERENCES

[1] Anderson, B. D. (1993, August). "Controller design: moving from theory to practice." *IEEE Control Systems Magazine, 13*(4), 16-25.

[2] Astrom, K. J., & Hagglund, T. (1995). "PID controllers, theory, design and tuning." *Instrument Society of America*.

[3] Astrom, K. J., & Wittenmark, B. (1997). *"Computer controlled systems."* Upper Saddle River, N.J.: Prentice Hall.

[4] Chen, T., & Qiu, L. (1994, July). "H∞ design of general multirate sampled-data control systems." *Automatica, 30*(7), 831-847.

[5] Cimino, C., & Pagilla, P. R. (2009, November). "A design technique for multirate linear systems." *IEEE Transactions on Control Systems Technology, 17*(6), 1342-1349.

[6] Costin, M. H., & Elzinga, D. R. (1989). "Active reduction of low-frequency tire impact noise using digital feedback control." *IEEE Control Systems Magazine, 9*(5), 3-6.

[7] Dorf, R. C., & Bishop, R. H. (2005). *"Modern control systems."* (10/E ed.). N.J.: Prentice Hall.

[8] Fujimoto, H., Hori, Y., & Kawamura, A. (2001, June). "Perfect tracking control based on multirate feedforward control with generalized sampling periods." *IEEE Transactions on Industrial Electronics, 48*(3), 636-644.

[9] Fujimoto, H., Kawamura, A., & Tomizuka, M. (1999, June). "Generalized digital redesign method for linear feedback system based on n-delay control." *IEEE/ASME Transactions on Mechatronics, 4*(2), 101-109.

[10] Glasson, D. P. (1983). "Development and applications of multirate digital control." *IEEE Control System Magazine, 3*(4), 2-8.

[11] Guo, S.-M., Shieh, L. S., Chen, G., & Lin, C.-L. (2000, November). "Effective chaotic orbit tracker: A prediction-based digital redesign approach." *IEEE Transactions on Circuits and Systems-I. Fundamental Theory and Applications, 47*(11), 1557-1570.

[12] Huang, C., Frederick, D., & Rimer, M. (1989, August). "CACSD benchmark problem no. 3." *IEEE Control Systems Magazine, 9*(5), 12-14.

[13] Kando, H., Yonemoto, Y., & Iwazumi, T. (1993). "Multi-rate regulator design of two-time-scale systems via digital redesign method." *International Journal of Systems Science, 24*(4), 691-706.

[14] Kranc, G. M. (1957). "Input-output analysis of multirate feedback systems." *IRE Transactions on Automatic Control, 3*(1), 21-28.

[15] Lee, S. H. (2006, January). "Multirate digital control system design and its application to computer disk drives." *IEEE Transactions on Control Systems Technology, 14*(1), 124-133.

[16] Li, Y., Yang, S. H., Zhang, Z., & Wang, Q. (2010). "Network load minimisation design for dual-rate Internet-based control systems." *IET Control Theory Appl., 4*(2), 197-205.

[17] Polites, M. E. (1989). "Ideal state reconstructor for deterministic digital control systems." *International Journal of Control, 49*(6), 2001-2012.

[18] Ralston, A., & Rabinowitz, P. (2001). *"A first course in numerical analysis."* (2 ed.). Dover Publications.

[19] Shieh, L. S., Chen , G., & Tsai, J. S. (1992). "Hybrid suboptimal control of multi-rate multi-loop sampled-data systems." *International Journal of Systems Science, 23*(6), 839-854.

[20] Shieh, L. S., Gu, J., & Bao, Y. L. (1993, November). "Model conversions of uncertain linear systems using the pade and inverse-pade method." *IEE Proceedings-D, Control Theory and Applications, 140*(6), 455-464.

[21] Shieh, L. S., Wang, W. M., & Panicker, A. (1998). "Design of pam and pwm digital controllers for cascaded analog systems." *ISA Transactions, 37*(3), 201-213.

[22] Trinh, H. (1999). "Linear Functional state observer for time-delay systems." *International Journal of Control, 72*(18), 1642-1658.

[23] Tsai, J. H., Chen, C. M., & Shieh, L. S. (1993, January). "Modelling of multirate feedback systems using uniform-rate models." *Applied Mathematical Modelling, 17*(1), 2-14.

[24] Tsay, Y. T., Shieh, L. S., & Tsai, J. S. (1986). "A fast method for computing the principal nth roots of complex matrices." *Applications of Linear Algebra, 76*, 205-221.

[25] Wang, H. P., Shieh, L. S., Tsai, J. S., & Zhang, Y. (2008, May). "Optimal digital controller and observer design for multiple time-delay transfer function matrices with multiple input-output delays." *International Journal of Systems Science, 39*(5), 461-476.

[26] Wang, H. P., Tsai, J. S., Yi, Y. I., & Shieh, L. S. (2004, April 10). "Lifted digital redesign of observer-based tracker for a sampled-data system." *International Journal of Systems Science, 35*(4), 255-271.

[27] Yang, L., & Yang, S. H. (2007, March). "Multi-rate control in internet based control systems." *IEEE Transactions on Systems, Man and Cybernetics-Part C: Applications and Reviews", 37*(2), 185-192.

Appendix A - Modeling Error of Direct Bilinear method for Singular A Matrices

The exact discretization of the continuous-time system in equations (2-1) and (2-2) with a piece-wise-constant input $u_c(t) = u_c(kT), kT \le t < kT + T$, can be described as

$$x_c(kT + T) = Gx_c(kT) + Hu_c(kT), \tag{A-1}$$

where $G = e^{AT}$ and $H = \int_{kT}^{kT+T} e^{(kT+T-\lambda)} B d\lambda = (G - I_n)A^{-1}B$ for a non-singular matrix A are the same matrices with equations (4-1) and (4-2). When the matrix A is a singular matrix, the matrix H can be evaluated as $H = \sum_{i=1}^{\infty} \frac{T}{i!}(AT)^{i-1}B$. Integrating both side of equation (4-1) yields

$$\int_{kT}^{kT+T} \dot{x}_c(t)\, dt = A \int_{kT}^{kT+T} x_c(t)\, dt + B \int_{kT}^{kT+T} u_c(t)\, dt. \tag{A-2}$$

Since $u_c(t) = u_c(kT)$ for $kT \le t < kT + T$, then the first integral term in the right-hand side of (A-2) can be approximately evaluated using the trapezoidal rule as $\int_{kT}^{kT+T} x_c(t)\, dt = \frac{T}{2}(x_c(kT + T) + x_c(kT))$. So equation (A-2) becomes

$$x_c(kT + T) - x_c(kT) = \frac{AT}{2}\big(x_c(kT + T) + x_c(kT)\big) + TBu_c(kT) \tag{A-3}$$

as above. Then the state-space model in equations (2-40) and (2-41) is obtained with $G_b = \left(I_n - \frac{AT}{2}\right)^{-1}\left(I_n + \frac{AT}{2}\right), H_b = (I_n - AT/2)^{-1}BT$. The Taylor series expansion of the system matrix $G = e^{AT}$ gives

$$
\begin{aligned}
G &= I_n + AT + \frac{1}{2}(AT)^2 + \sum_{i=3}^{\infty} \frac{1}{i!}(AT)^i \\
&\cong I_n + AT + \frac{1}{2}(AT)^2 + \sum_{i=3}^{\infty} \frac{1}{2^{i-1}}(AT)^i \\
&= I_n + AT + \frac{1}{2}\left[I_n - \left(\frac{1}{2}AT\right)\right]^{-1} \\
&= \left[I_n - \left(\frac{1}{2}AT\right)\right]^{-1}\left[I_n + \left(\frac{1}{2}AT\right)\right] \\
&= G_b
\end{aligned} \tag{A-4}
$$

for $\left\|\frac{1}{2}AT\right\| < 1$. The approximated input vector $H = (G - I_n)A^{-1}B$ gives

$$
H = (G - I_n)A^{-1}B \cong (G_b - I_n)A^{-1}B = \left(I_n - \left(\tfrac{1}{2}AT\right)\right)^{-1} BT = H_b. \tag{A-5}
$$

Define the system modeling error matrix $E_g = e^{AT} - G_b$ for the open-loop bilinear system model equations (2-40) and (2-41), then $E_g = \sum_{i=1}^{\infty}\left(\frac{1}{i!} - \frac{1}{2^{i-1}}\right)(AT)^i$ is obtained. Since $\frac{1}{i!} - \frac{1}{2^{i-1}} < 0$ for i ≥ 3, then

$$
\left\|E_g\right\| = \left\|e^{AT} - G_b\right\| \le \sum_{i=1}^{\infty}\left(\frac{1}{i!} - \frac{1}{2^{i-1}}\right)\left\|(AT)^i\right\| = \frac{1+0.5\|AT\|}{1-0.5\|AT\|} - e^{\|AT\|} \tag{A-6}
$$

is obtained for $T \le \frac{2}{\|A\|}$.

Similarly, The input modeling error vector (denoted as E_b) for the open-loop bilinear system model in equations (2-40) and (2-41) is

$$E_b = (G - I_n)A^{-1}B - \left(I_n - \left(\frac{1}{2}AT\right)\right)^{-1} BT$$

$$= \sum_{i=1}^{\infty} \left(\frac{1}{i!} - \frac{1}{2^{i-1}}\right)(AT)^i BT$$

$$= \left(\sum_{i=1}^{\infty} \left(\frac{1}{i!} - \frac{1}{2^{i-1}}\right)(AT)^i\right) A^{-1}B = E_g A^{-1}B. \quad \text{(A-7)}$$

Hence, the modeling error value becomes

$$\|E_b\| \leq \|E_g\| \|A^{-1}B\| \leq \|E_g\| \|A\|^{-1} \|B\| \quad \text{(A-8)}$$

for $T \leq \frac{2}{\|A\|}$ and a non-singular matrix A. If the matrix A is singular, the modeling error value $\|E_b\|$ becomes

$$\|E_b\| \leq (\sum_{i=1}^{\infty} (\frac{1}{2^{i-1}} - \frac{1}{i!}) \|AT\|^{i-1}) \|B\| T. \quad \text{(A-9)}$$

Appendix B - Exact Evaluation of Discrete-time Model

Consider the continuous-time signal expressed in state space model as below

$$\dot{x}(t) = Ax(t) + Bu(t), x(0) = \propto, \quad \text{(B-1)}$$

and $u(t) = u(kT)$ for $kT \leq t < kT + T$.

Assume that $x(t) = e^{AT} f(t)$, then the derivative of x(t) follows

$$\dot{x}(t) = Ae^{At} f(t) + e^{At} \dot{f(t)}$$

$$= Ax(t) + e^{At} f(\dot{t}), \tag{B-2}$$

as shown above. Comparing equations (B-1)and (B-2), it is concluded that $e^{AT} f(\dot{t}) = Bu(t)$. Integrating $f(\dot{t})$ from -∞ to t is derived as below

$$f(\dot{t}) = e^{-At} Bu(t), \tag{B-3}$$

$$f(t) = \int_{-\infty}^{t} e^{-A\lambda} Bu(\lambda) d\lambda, \tag{B-4}$$

Replacing equation (B-4) with the assumption that was made for x(t) follows as

$$x(t) = e^{At} f(t) = e^{At} \int_{-\infty}^{t} e^{-A\lambda} Bu(\lambda) d\lambda$$

$$= e^{At} \left[\int_{-\infty}^{0} e^{-A\lambda} Bu(\lambda) d\lambda + \int_{0}^{t} e^{-A\lambda} Bu(\lambda) d\lambda \right]$$

$$= e^{At} x(0) + \int_{0}^{t} e^{-A(t-\lambda)} Bu(\lambda) d\lambda \tag{B-5}$$

shown above.

Equation (B-5) is one of the fundamental equations used to derive the exact discrete-time modeling. Substituting two different time intervals t=kT and t=kT+T leads to the discrete-time model as follows. For t=kT

$$x(kT) = e^{kAT} x(0) + \int_{0}^{kT} e^{A(kT-\lambda)} Bu(\lambda) d\lambda, \tag{B-6}$$

and for t=kT+T

$$x(kT+T) = e^{A(kT+T)}x(0) + \int_0^{kT+T} e^{A(kT+T-\lambda)}\,Bu(\lambda)d\lambda$$

$$= e^{AT}\left[e^{kAT}x(0) + \int_0^{kT} e^{A(kT-\lambda)}\,Bu(\lambda)d\lambda\right] + \int_{kT}^{kT+T} e^{A(kT+T-\lambda)}\,Bd\lambda u(kT)$$

$$= e^{AT}x(kT) + [e^{AT} - I_n]A^{-1}Bu(kT)$$

$$= Gx(kT) + Hu(kT), \qquad \text{(B-7)}$$

is as shown above, where $G = e^{AT}$ and $H = (G - I_n)A^{-1}B$.